

Copyright © 2021

RBOT101: Mathematical Foundations of Robotics

Instructor: Dr. Olalekan Ogunmolu

All rights reserved

## TABLE OF CONTENTS

LIST OF FIGURES . . . . .	iv
LIST OF TABLES . . . . .	v
CHAPTER 1 PREAMBLE . . . . .	1
1.1 Course Description . . . . .	1
1.2 Course Outcomes . . . . .	1
1.3 Prerequisites . . . . .	2
1.4 Recommended Texts . . . . .	2
1.5 Recommended Journals . . . . .	3
1.6 Required Software . . . . .	3
1.7 Online Course Content . . . . .	3
1.8 Assessments and Labs . . . . .	4
1.9 Errata . . . . .	4
CHAPTER 2 OBJECTS' ALIGNMENT IN ROBOTICS. . . . .	5
2.1 Preliminaries . . . . .	6
2.1.1 Distance between a Point and a Parameterized Entity . . . . .	8
2.1.2 Distance between a Point and an Implicit Entity . . . . .	10
2.1.3 Quaternions . . . . .	11
2.2 Closed-form Solution using Least Sum of Squares Errors . . . . .	12
2.2.1 Kabsch Algorithm . . . . .	13
2.2.2 Examples . . . . .	15
2.2.3 Corresponding Point Set Registration with Quaternions . . . . .	20
2.3 Iterative Closest Point . . . . .	24
CHAPTER 3 RIGID BODY MOTIONS: INTRODUCTION . . . . .	25
3.1 Robots Components . . . . .	26
3.2 Robot Spaces, Geometries, and Classifications . . . . .	27
3.3 Characterization of Kinematic Geometry . . . . .	28
3.3.1 Kinematic Geometries . . . . .	28
3.3.2 Open Kinematic Chains . . . . .	29

3.3.3	Closed-loop Kinematic Chains . . . . .	31
3.4	Freedom and Structure in Mechanisms . . . . .	32
3.4.1	Freedom, Connectivity and Mobility . . . . .	32
3.4.2	Constraints and Freedoms . . . . .	34
3.4.3	The Mobility Criterion . . . . .	35
CHAPTER 4	MOTION OF RIGID BODIES . . . . .	38
4.1	Screws . . . . .	38
4.1.1	Motion screws: Twist's Pitch, Axis, and Magnitude . . . . .	39
4.1.2	Dynamics Screws: Twist's Pitch, Axis, and Magnitude . . . . .	41
4.1.3	Screw Motions . . . . .	42
4.2	Rodrigues' Formula . . . . .	42
4.3	The Matrix Exponential, The Lie Group and Lie Algebra . . . . .	43
4.3.1	The Lie Group Notations . . . . .	46
4.3.2	Exponential Map and Kinematic Chains . . . . .	47
4.4	Rigid Body Transformations . . . . .	47
4.4.1	Translation in $\mathbb{R}^3$ . . . . .	49
4.4.2	Rotations in $\mathbb{R}^3$ . . . . .	51
4.4.3	Rotation Matrices as Transformations . . . . .	53
4.4.4	Planar Rotations . . . . .	54
4.4.5	Composition of Rotations . . . . .	57
4.5	Parameterization of Rotations $\in SO(3)$ . . . . .	60
4.5.1	Axis-Angle Parameterizations . . . . .	60
4.5.2	Euler Angles . . . . .	61
4.5.3	Quaternions . . . . .	64
4.6	Homogeneous Coordinates . . . . .	64
4.7	Rigid Body Velocities . . . . .	66
4.7.1	Rotational Velocities . . . . .	66
4.7.2	Rigid Body Velocity . . . . .	68
REFERENCES	. . . . .	70

## LIST OF FIGURES

2.1 Given two coordinate systems, we measure a number of points in the two different coordinate systems. The goal is to find the transformation between the two points. . . . .	12
3.1 Early serial kinematic chain robot manipulators. <i>Left:</i> The Stanford Arm Serial Manipulator, 1969. ©Infolab, Stanford University. <i>Right:</i> The PUMA robot arm. Reprinted from Wikipedia. . . . .	25
3.2 Soft Robot Manipulators <i>Left:</i> An octopus inspired soft robot. Robots classified under muscular hydrostats. ©Cecilia Laschi. <i>Right:</i> A soft parallel robot manipulator (Hopkins et al., 2015). . . . .	26
3.3 Schematic description of in-series-actuated robot arms: (a) rotary joint actuated “about” the hinge (b) prismatic joint actuated “across” a hinge. Reprinted from (Hunt, 1983). . . . .	29
3.4 The Staubli 6-DOF Arm is an example of a Spherical Manipulator. Reprinted from DirectIndustry’s Webpage. . . . .	30
3.5 The SCARA Arm. ©Fanuc America. . . . .	30
3.6 Stewart-Gough Platforms <i>Left:</i> The 1954 Octahedral hexapod of the original Gough platform. <i>Right:</i> The retired platform from Dunlop tires in 2000. Picture courtesy of Parallemic.org. . . . .	32
3.7 The Lower Kinematic Pairs. Reprinted from (Hunt, 1977). . . . .	33
3.8 The planar <i>RRR</i> linkage, ( <i>left</i> ) is modified in ( <i>right</i> ) to allow spatial spin-movement of the coupler 3; the connectivity $\mathcal{C}_{13} = 2$ . Reprinted from (Hunt, 1977). . . . .	34
3.9 <i>Left:</i> A Parallel Planar Robot Mechanism. <i>Right:</i> Workspace of the mechanism. . . . .	37
4.1 Illustration of rotation of interconnecting link of two spherical links. . . . .	44
4.2 Lie Group and their Notations. Reprinted with permission from Federico Renda. IROS 2018, Screw Theory Tutorial. . . . .	46
4.3 An illustration of the exponential map for a multi-body rigid system. Reprinted with permission from Federico Renda. IROS 2018, Screw Theory Tutorial. . . . .	48
4.4 A point $q$ in space with respect to two coordinate frames. . . . .	50
4.5 An illustration of the relative orientation of a rigid object $q$ between an inertial frame $I$ and a body frame $J$ . . . . .	52
4.6 Illustration of rotation between two frames in a plane. . . . .	55
4.7 Relative orientation between two frames. . . . .	56
4.8 Coordinate frames on a body. Reprinted from (Spong et al., 2006) . . . . .	58
4.9 Illustration of composition of rotations about a <b>current axis</b> . . . . .	60
4.10 An illustration of the ZYZ rotation angles . . . . .	62

## LIST OF TABLES

## **CHAPTER 1**

### **PREAMBLE**

Consider this the roadmap for this course. Please read through the syllabus posted on Moodle2 carefully and feel free to share any questions that you may have. Please print a copy of the Syllabus for reference. Some relevant parts of the Syllabus are repeated here but the Moodles reference should serve as your guide throughout the ten weeks of this course.

#### **1.1 Course Description**

This course focuses on the algorithmic and mathematical concepts with respect classical and recent methods for solving real-world problems in robotics. While some students may have encountered some of the concepts we will be treating in past courses or avenues of study, we will provide the breadth and depth necessary for equipping students to be world-class roboticists. The topics covered by this course shall include the configuration space, rigid bodies, semi-rigid soft bodies, as well as their motions in  $\mathbb{R}^n$ , wrenches, homogeneous transformations, optimal algorithms for rigid body rotations, linear systems theory, probability theory, the Kalman filter. The course will begin and end with a self-assessment to allow students to gauge their strengths and weaknesses in these topics. References for further, in-depth study in each topic are provided at the end of this course.

#### **1.2 Course Outcomes**

After taking this course, each student will be able to

- Develop mathematical tools for solving fundamental kinematic problems in robot operation;
- Formulate optimal state estimation tools for solving real-time smoothing and filtering operations in robotics;

- Integrate state estimation with rigid and semi-rigid soft bodies to solve real-world automation problems; and 4. Use open-source Python, and C++ tools to solve classical and emerging problems in robotics in our day.

### 1.3 Prerequisites

An undergraduate-level understanding of linear algebra, analytical mechanics, Python and C++ programming.

### 1.4 Recommended Texts

- Main Texts
  - Simon, Dan. (2007). Optimal state estimation: Kalman,  $H = \infty$ , and nonlinear approaches. Choice Reviews Online, Vol. 44, pp. 44-3334-443334. <https://doi.org/10.5860/choice.44.3334>
  - Murray, R. M., Li, Z., and Sastry, S. S. (1994). A Mathematical Introduction to Robotic Manipulation. Book (Vol. 29). Free PDF preprint downloadable from, [Murray's website](#).
  - Theory of Screws: A Study in the Dynamics of a Rigid Body by Robert Stawell Ball, Dublin: Hodges, Foster, and Co., Grafton-Street. a. Textbooks:
- Secondary Text
  - Modern Robotics: Mechanics, Planning, and Control. Free PDF preprint downloadable from [Author's Northwestern University Website](#).
- Auxiliary Text:

- Theory of Screws: A Study in the Dynamics of a Rigid Body by Robert Stawell Ball, Dublin: Hodges, Foster, and Co., Grafton-Street (Should be downloadable via Interlibrary Loan).

## 1.5 Recommended Journals

- [IEEE Transactions on Robotics](#).
- [The International Journal of Robotics Research](#).
- [The IEEE International Conference on Robotics and Automation \(ICRA\)](#).
- [IEEE/Robotics Society of Japan International Conference on Intelligent Robots and Systems \(IROS\)](#).
- [Robotics and Autonomous Systems, An Elsevier Journal](#).

## 1.6 Required Software

- A working knowledge of python and the anaconda environment.
- ROS 1.x Installation Instructions: [ros 1.x website](#).
- ROS 2 installation [ros 2.0 website](#).

## 1.7 Online Course Content

This course will be conducted completely online using Brandeis LATTE [site](#). The site contains the course syllabus, assignments, our discussion forums, links/resources to course-related professional organizations and sites, and weekly checklists, objectives, outcomes, topic notes, self-tests, and discussion questions. Access information is emailed to enrolled participants before the start of the course. To begin participating in the course, review the “Welcoming Message” and the “Week 1 Checklist.”

## **1.8 Assessments and Labs**

Please read the syllabus posted on the RBOT 101 website thoroughly.

## **1.9 Errata**

If in the course of using these notes, you find sentence errors, errata or mistakes in equations, please annotate them and upload it to the discussion forum. Points will awarded, at the discretion of the instructor, for such help.

## CHAPTER 2

### OBJECTS' ALIGNMENT IN ROBOTICS.

In this chapter, we are concerned with the problem of optimally aligning two vectors, a model point/shape to a “sensed” or measured point/shape in space e.g.  $\nu_1, \nu_2 \in \mathbb{R}^n$  to one another with the minimal amount of errors. To transform between two points in the Cartesian coordinate system is akin to the problem of solving a rigid body motion problem where that yields a rotation and a translation. In addition, the scaling factor may be unknown. For translation, there are three degrees of freedom, while rotation has another three viz., the direction of the axis about which we are rotating, the angle of rotation itself, and the scaling. Three points in either coordinate systems give us nine constraints (with each contributing three coordinates), more than enough to find the seven unknowns. If we discard two of the constraints, we end up with seven equations in seven unknowns that can be developed to allow us to recover the parameters.

There exists many methods of solving this problem. Most of them leverage clever optimization methods and we will be looking into these in this chapter. We could follow the homogeneous transformation scheme we presented in Chapter 1, but we would not have an optimal solution. A popular technique in computer geometry and computer vision is to use the iterative closest point algorithm(ICP), an algorithm by Paul Besl and Neil McKay developed out of General Motors Laboratory in the 1990’s ([Besl and McKay, 1992](#)). This is more appropriate for 3D tasks and it describes a generic, representation method for the accurate and computationally efficient registration of three-dimensional (3-D) shapes. The ICP algorithm always converges monotonically to the nearest local minimum of a mean-square distance metric such as an  $l_2$  distance, and this convergence rate is of the order of a few iterations. An important property of the ICP algorithm is that it can register data from unfixed rigid objects with an ideal geometrical model prior to shape inspection. So, if we want to figure out that two geometric representations are congruent, estimate the motion between them in real-time where the correspondences are not known, ICP tends to be really good for such operations.

Now, suppose our dataset is not a complex geometric primitive<sup>1</sup>, but rather a set of two vectors such that we are tasked with the problem of determining the best *unconstrained transformation* between the two sets of coordinates. We can formulate the problem into a constrained optimization problem and thereafter, through clever factorization, turn the problem into a simple one of factorizing the unconstrained transformation into a symmetric and orthogonal matrix by which we may solve for the optimal rotation and translation. The algorithm we shall be looking into will be the one that was invented in crystallography in 1976 and updated in 1978 by Wolfgang Kabsch, today dubbed the Kabsch algorithm (Kabsch, 1978). Kabsch showed that a direct solution was possible, irrespective of the non-linear character of the problem.

While other newer algorithms exist, these are the two popular algorithms that we shall be concerning ourselves with in this chapter.

## 2.1 Preliminaries

We will denote the real line by  $\mathbb{R}$ . An example of a **metric space** is the **Euclidean  $n$ -space**  $\mathbb{R}^n$ , which consists of  $n$ -tuples  $x = (x_1, x_2, \dots, x_n)$  where each  $x_i \in \mathbb{R}$ . We shall mean an  $\mathbb{R}^n$  metric space to have the metric

$$d(x, y) = \sqrt{\sum_{i=1}^n (y_i - x_i)^2}. \quad (2.1.1)$$

If  $n = 0$ , then  $\mathbb{R}^0$  is taken to be a single point  $0 \in \mathbb{R}$ .

A manifold is “locally” similar to one of the example metric spaces  $\mathbb{R}^n$ . Precisely, a **manifold** is a metric space  $M$  with the property that, if  $x \in M$ , then there is some neighborhood  $U$  of  $x$  and some integer  $n \geq 0$  such that  $U$  is homeomorphic<sup>2</sup> to  $\mathbb{R}^n$ .

<sup>1</sup>We shall refer to a geometric primitive as a primitive 3D shape such as a cylinder, square, prism and the likes.

<sup>2</sup>A homeomorphic mapping means intrinsic topological equivalence between e.g. objects. Two objects are homeomorphic if they can be deformed into each other by a continuous, invertible mapping. Such a homeomorphism ignores the space in which surfaces are embedded, so the deformation can be completed in a higher dimensional space than the surface was originally embedded. Mirror images are homeomorphic, as are Möbius strip with an even number of half-twists, and Möbius strip with an odd number of half-twists (Weisstein, Weisstein).

A simple example of a manifold is  $\mathbb{R}^n$ : for each  $x \in \mathbb{R}^n$  we can take  $U$  to be everything in  $\mathbb{R}^n$ .

**Quiz 1.** Suppose we supply  $\mathbb{R}^n$  with an equivalent metric, which makes it homeomorphic to  $\mathbb{R}^n$ , would it also be a manifold?

Another example of a metric space is an open ball in  $\mathbb{R}^n$ , wherein one can take  $U$  to be the entire open ball since an open ball in  $\mathbb{R}^n$  is homeomorphic to  $\mathbb{R}^n$ . Similarly, an open subset  $V$  of  $\mathbb{R}^n$  is a manifold, *i.e.* for each  $x \in V$  we can choose  $U$  to be some open ball with  $x \in U \subset V$ .

The **Euclidean distance**  $d(\mathbf{r}_1, \mathbf{r}_2)$  between two points  $\mathbf{r}_1 = (x_1, y_1, z_1)$  and  $\mathbf{r}_2 = (x_2, y_2, z_2)$  is given by

$$d(\mathbf{r}_1, \mathbf{r}_2) = \|\mathbf{r}_1 - \mathbf{r}_2\| = \sqrt{(x_2 - x_1)^2 + (y_2 - y_1)^2 + (z_2 - z_1)^2}. \quad (2.1.2)$$

Suppose that  $P$  is a point set with  $N_p$  points denoted as  $\mathbf{p}_i : P = \{\mathbf{p}_i\}$  for  $i = 1, \dots, N_p$ . The distance between the point  $\mathbf{q}$  and the point set  $P$  is

$$d(\mathbf{q}, P) = \min_{i \in \{1, \dots, N_p\}} d(\mathbf{q}, \mathbf{p}_i). \quad (2.1.3)$$

We find that the closest point  $\mathbf{p}_j$  of  $P$  satisfies  $d(\mathbf{q}, \mathbf{p}_j) = d(\mathbf{q}, P)$ .

Suppose that we have a **line segment** that connects the points,  $bmr_1, \mathbf{r}_2$ , the distance between the point  $\mathbf{r}$  and the line segment  $l$  is

$$d(\mathbf{p}, l) = \min_{x+y=1} \|x\mathbf{r}_1 + y\mathbf{r}_2 - \mathbf{p}\| \quad (2.1.4)$$

where  $x, y \in [0, 1]$ .

**Homework 1.** Find a closed-form expression for the solution to (2.1.4).

Now, if instead of a line segment, suppose we have a set of  $N_l$  line segments denoted  $l_i$ , and let  $L = \{l_i\}$  for  $i = 1, \dots, N_l$ . The **distance between the point  $\mathbf{p}$  and the line segment set  $L$**  is

$$d(\mathbf{p}, L) = \min_{i \in \{1, \dots, N_l\}} d(\mathbf{p}, l_i). \quad (2.1.5)$$

The closest point  $y_j$  on the line segment set  $L$  satisfies  $d(\mathbf{p}, y_j) = d(\mathbf{p}, L)$ . Let  $g$  be a triangle with the following coordinates  $\mathbf{r} = (x_1, y_1, z_1)$ ,  $\mathbf{r}_2 = (x, y, z)$ , and  $\mathbf{r}_3 = (x_3, y_3, z_3)$ . The **distance between the point  $p$  and the triangle  $g$**  is

$$d(\mathbf{p}, g) = \min_{x+y+z=1} \|x\mathbf{r}_1 + y\mathbf{r}_2 + z\mathbf{r}_3 - \mathbf{p}\| \quad (2.1.6)$$

where  $x \in [0, 1]$ ,  $y \in [0, 1]$ , and  $z \in [0, 1]$ .

**Homework 2.** Find a closed-form expression for the problem in (2.1.6).

Now, if we have a collection of  $N_g$  triangles  $G$ , denoted by  $g_i$  such that  $G = \{g_i\}$  for  $i = 1, \dots, N_g$ . The **distance between the point  $p$  and the triangle set  $G$**  is

$$d(\mathbf{p}, G) = \min_{i \in \{1, \dots, N_g\}} d(\mathbf{p}, g_i), \quad (2.1.7)$$

and the closest point  $y_j$  on the triangle set  $G$  satisfies the equality  $d(\mathbf{p}, y_j) = d(\mathbf{p}, G)$ .

### 2.1.1 Distance between a Point and a Parameterized Entity

We define a parametric curve and a parametric surface as single parametric entities  $\mathbf{r}(\mathbf{u})$ , where  $\mathbf{u} = u \in \mathbb{R}^1$  denotes a parameterized curve, and  $\mathbf{u} = (u, v) \in \mathbb{R}^2$  denotes parametric surfaces. We will evaluate a curve within an interval domain e.g.  $[x, y]$  while the evaluation domain of a surface can be an arbitrarily closely-connected region in a plane.

We will take the distance from a given point  $\mathbf{p}$  to a parametric entity  $E$  to be

$$d(\mathbf{p}, E) = \min_{\mathbf{r}(\mathbf{u}) \in E} d(\mathbf{p}, \mathbf{r}(\mathbf{u})) \quad (2.1.8)$$

To compute the point-to-curve and point-to-surface distances, let  $F$  be the set of  $N_e$  parametric entities denoted by  $E_i$ , and let  $F = \{E_i\}$  for  $i = 1, N_e$ . The distance between a point  $\mathbf{p}$  and the parametric entity set  $F$  is

$$d(\mathbf{p}, F) = \min_{i \in \{1, \dots, N_e\}} d(\mathbf{p}, E_i). \quad (2.1.9)$$

To find the distance from a point to a parametric entity, we can create a simplex-based approximation for e.g. a line segment or triangle. For a parametric space curve  $C = \{\mathbf{r}(u)\}$ , we can compute a polyline  $L(C, \delta)$  such that the piecewise-linear approximation never deviates from the space curve by more than a prespecified distance  $\delta$ . If we tag every point of the polyline with a corresponding  $u$  argument values of the parametric curve, we can obtain an estimate of the closest point from the line segment set.

In a similar vein, for a parametric surface  $S = \{\mathbf{r}(u, v)\}$ , one can compute a triangle set  $G(S, \delta)$  such that the piecewise triangular approximation never deviates from the surface by more than a prespecified distance  $\delta$ . If we tag each triangle vertex with the corresponding  $(u, v)$  argument values of the parametric surface, we can find the  $U_a, V_a$  of the argument values of the closest point from the triangle set. The initial value of  $\mathbf{u}_a$  is assumed to be available such that  $\mathbf{r}(\mathbf{u}_a)$  is very close to the closest point on the parametric entity.

We can employ a Newtonian minimization approach for solving the point to parametric entity problem when a reliable starting point  $\mathbf{u}_a$  is available. The scalar objective function to be minimized is

$$f(\mathbf{u}) = \|\mathbf{r}(\mathbf{u}) - \mathbf{p}\|^2. \quad (2.1.10)$$

Suppose  $\Delta = [\partial/\partial \mathbf{u}]^T$  is the vector differential gradient operator, the minimum of  $f$  must occur at  $\Delta f = 0$ . If we have a surface, then we must have  $\Delta f = [f_u, f_v]^T$ , with the 2-D Hessian matrix is given by

$$\Delta\Delta^T(f) = \begin{bmatrix} f_{uu} & f_{uv} \\ f_{uv} & f_{vv} \end{bmatrix} \quad (2.1.11)$$

where the partial derivatives of the objective function is

$$f_u(\mathbf{u}) = 2\mathbf{r}_u^T(\mathbf{u})(\mathbf{r}(\mathbf{u}) - \mathbf{p}) \quad (2.1.12a)$$

$$f_v(\mathbf{u}) = 2\mathbf{r}_v^T(\mathbf{u})(\mathbf{r}(\mathbf{u}) - \mathbf{p}) \quad (2.1.12b)$$

$$f_{uu}(\mathbf{u}) = 2\mathbf{r}_{uu}^T(\mathbf{u})(\mathbf{r}(\mathbf{u}) - \mathbf{p}) + 2\mathbf{r}_u^T(\mathbf{u})\mathbf{r}_u(\mathbf{u}) \quad (2.1.12c)$$

$$f_{vv}(\mathbf{u}) = 2\mathbf{r}_{vv}^T(\mathbf{u})(\mathbf{r}(\mathbf{u}) - \mathbf{p}) + 2\mathbf{r}_v^T(\mathbf{u})\mathbf{r}_v(\mathbf{u}) \quad (2.1.12d)$$

$$f_{uv}(\mathbf{u}) = 2\mathbf{r}_{uv}^T(\mathbf{u})(\mathbf{r}(\mathbf{u}) - \mathbf{p}) + 2\mathbf{r}_u^T(\mathbf{u})\mathbf{r}_v(\mathbf{u}). \quad (2.1.12e)$$

And the update relation for the curve and surface case is

$$\mathbf{u}_{k+1} = \mathbf{u}_k - [\Delta\Delta^T(f)(\mathbf{u}_k)]^{-1} \Delta f(\mathbf{u}_k) \quad (2.1.13)$$

where  $\mathbf{u}_0 = \mathbf{u}_a$ .

### 2.1.2 Distance between a Point and an Implicit Entity

An implicit geometric entity is the zero set of a possibly vector-valued multivariate function  $\mathbf{g}(\mathbf{r}) = 0$ . Examples of this distance could be a point-to-curve or point-to-surface distance. The important thing to bear in mind is that the distance metric for an individual entity, once defined, makes the sets of implicit entities straightforward to implement. The distance from a given point  $\mathbf{p}$  to an implicit entity  $I$  is given by

$$d(\mathbf{p}, I) = \min_{\mathbf{g}(\mathbf{r})=0} d(\mathbf{p}, \mathbf{r}) = \min_{\mathbf{g}(\mathbf{r})=0} \|\mathbf{r} - \mathbf{p}\|. \quad (2.1.14)$$

It is helpful to note that when computing the implicit entity distance from a point, the solution is never closed-form and are usually involved. Suppose that  $J$  is the set of  $N_I$  parametric entities, represented by  $I_k$  and  $J = \{I_k\}$  for  $k = 1, N_I$ . The distance between a point  $\mathbf{p}$  and the implicit entity set  $J$  is given by

$$d(\mathbf{p}, J) = \min_{k \in \{1, \dots, N_I\}} d(\mathbf{p}, I_k), \quad (2.1.15)$$

and the closest point  $\mathbf{y}_j$  on the implicit entity  $I_j$  satisfies the equality  $d(\mathbf{p}, \mathbf{y}_j) = d(\mathbf{p}, J)$ . In order to compute the distance from a point to an implicit entity, we can create a simplex-based approximation such as line segments or triangles. The point-to-line or point-to-triangle set distance yields an approximate closest point  $\mathbf{r}_a$  which can be used to compute the exact distance.

Typically, we must solve a constrained optimization problem when finding the closest point on an implicit entity, say  $\mathbf{g}(\mathbf{r}) = 0$  to a point  $\mathbf{p}$  in order to minimize a quadratic objective function that is subject to a nonlinear constraint

$$\min f(\mathbf{r}) = \|\mathbf{r} - \mathbf{p}\|^2 \quad (2.1.16)$$

where  $\mathbf{g}(\mathbf{r}) = 0$  We can form the augmented Lagrange multiplier system of equations to solve the above, *i.e.*

$$\begin{aligned} \Delta f(\mathbf{r}) + \boldsymbol{\lambda}^T \Delta \mathbf{g}(\mathbf{r}) &= 0 \\ \mathbf{g}(\mathbf{r}) &= 0 \end{aligned} \quad (2.1.17)$$

where  $\Delta = [\partial/\partial \mathbf{r}]^T$ .

### 2.1.3 Quaternions

The unit quaternion is a four vector  $\mathbf{q}_R = [q_0, q_1, q_2, q_3]^T$ , where  $q_0 \geq 0$ , and  $q_0^2 + q_1^2 + q_2^2 + q_3^2 = 1$ , used to parameterize a rotation matrix. The  $3 \times 3$  rotation matrix generated by a unit rotation quaternion is given by

$$R = \mathbf{q}_R^T \mathbf{q}_R = \begin{bmatrix} q_0^2 + q_1^2 - q_2^2 - q_3^2 & 2(q_1 q_2 - q_0 q_3) & 2(q_1 q_3 + q_0 q_2) \\ 2(q_1 q_2 + q_0 q_3) & q_0^2 + q_1^2 - q_2^2 - q_3^2 & 2(q_2 q_3 - q_0 q_1) \\ 2(q_1 q_3 + q_0 q_2) & 2(q_2 q_3 + q_0 q_1) & q_0^2 + q_3^2 - q_1^2 - q_2^2 \end{bmatrix} \quad (2.1.18)$$

For more on unit quaternions, see § 4.5.3.

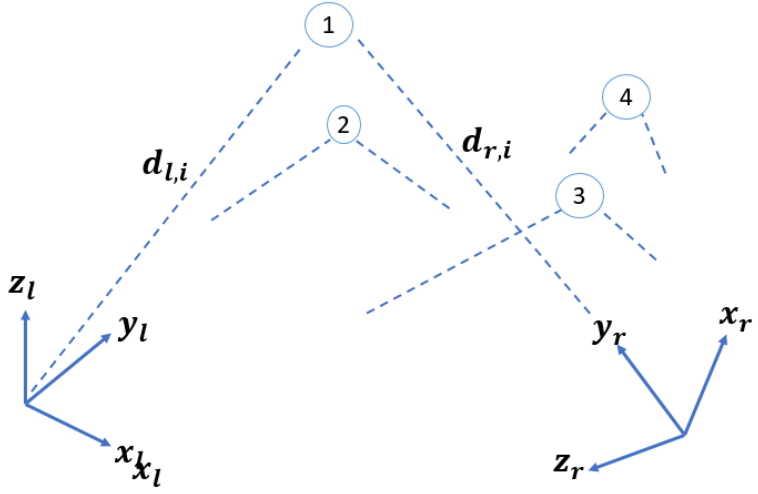


Figure 2.1: Given two coordinate systems, we measure a number of points in the two different coordinate systems. The goal is to find the transformation between the two points.

## 2.2 Closed-form Solution using Least Sum of Squares Errors

As we will see from our sensors, measurements are often inexact, which means we need a way to enforce greater accuracy when determining the transformation parameters. Therefore, we will need more than three points. One approach is to minimize the sum of squares of residual errors using various empirical, graphical, and numerical procedures. Because these are iterative in nature, they lead to an approximate solution and while the answer is better, it is imperfect. Iterative methods are repeatedly applied until the residual error is negligible.

There are closed-form solutions which present the absolute orientation in a single step with the best possible transformation given the measurements of the points in the two coordinate systems (Horn, 1987; Kabsch, 1978). With these closed-form least sum of squares methods, we do not need to find an initial good guess as is the case for iterative methods.

### 2.2.1 Kabsch Algorithm

Suppose we have two sets of vectors  $\mathbf{x}_n$  and  $\mathbf{y}_n$  where  $n = 1, \dots, N$ , and weight  $w_n$  that corresponds to each pair  $\mathbf{x}_n$  and  $\mathbf{y}_n$ . Our goal is to find an orthogonal matrix  $\mathbf{U} = (u_{ij})$  which minimizes the cost function

$$C = \frac{1}{2} \sum_n w_n (\mathbf{U} \mathbf{x}_n - \mathbf{y}_n)^2 \quad (2.2.1)$$

subject to

$$\sum_k u_{ki} u_{kj} - \delta_{ij} = 0 \quad (2.2.2)$$

where  $\delta_{ij}$  are the elements of a unit matrix. When there is a translation, we can find the centroid of the vector sets to the origin.

In order to solve the problem, we may introduce a symmetric Lagrangian matrix of multipliers,  $L = (l_{ij})$  and an auxiliary function as follows

$$D = \frac{1}{2} \sum_{i,j} l_{ij} (\sum_k u_{ki} u_{kj} - \delta_{ij}) \quad (2.2.3)$$

so that we can form the Lagrangian,  $E = C + D$ . For each condition in [eq. 2.2.2](#), we have an independent number  $l_{ij}$  so that the constrained minimum of  $C$  is part of the free minima of  $D$ . A free minimum of  $D$  can occur if

$$\frac{\partial E}{\partial u_{ij}} = \sum_k u_{ik} (\sum_n w_n x_{nk} x_{nj} + l_{k,j}) - \sum_n w_n y_{nl} x_{nj} = 0 \quad (2.2.4)$$

and

$$\frac{\partial^2 E}{\partial u_{mk} \partial u_{ij}} = \delta_{mi} (\sum_n w_n x_{nk} x_{nj} + l_{k,j}) \quad (2.2.5)$$

are elements of a positive definite matrix  $x_{nk}$  and  $y_{nk}$  are the  $k$ th elements of  $\mathbf{x}_n$  and  $\mathbf{y}_n$ . Now, suppose we have a matrix  $R = (r_{ij})$  and a symmetric matrix  $S = (s_{ij})$ , such that

$$r_{ij} = \sum_n w_n y_{ni} x_{nj} \quad (2.2.6)$$

and

$$s_{ij} = \sum_n w_n x_{ni} x_{nj}. \quad (2.2.7)$$

If the matrix (2.2.5) has 1 along its diagonal, we must have the minimum of the Lagrangian E to mean that  $S + L$  is positive definite, and (2.2.4) translates to

$$U.(S + L) = R. \quad (2.2.8)$$

Our goal would be to find a matrix  $L$  of Lagrange multipliers so that  $\cup$  is orthogonal. We can do this by multiplying both sides of (2.2.8) by their transposed matrices so that we can get rid of matrix  $\cup$  as follows:

$$\begin{aligned} U(S + L)^T(S + L) &= (S + L)^T U^T U(S + L) \\ &= (S + L)(S + L) = R^T R. \end{aligned} \quad (2.2.9)$$

Now, we know that  $R^T R$  is a symmetric positive definite matrix so that we can find the eigenvalues  $\lambda_k$  and eigenvectors  $\mathbf{v}_k$  using standard procedures e.g. single value decomposition. Thus, since  $S + L$  is symmetric and positive definite, it must have normalized eigenvectors,  $\mathbf{v}_k$  and positive eigenvalues  $\sqrt{\lambda_k}$  so that the Lagrange multipliers are

$$l_{ij} = \sum_k \sqrt{\lambda_k}; \quad \mathbf{v}_{ki} \mathbf{v}_{ki} - s_{ij} \quad (2.2.10)$$

where  $\mathbf{v}_{ki}$  signifies the  $i$ th component of  $\mathbf{v}_k$  and the effect of the orthogonal matrix  $U$  on these eigenvectors  $\mathbf{a}_k$  is determined from (2.2.8) which defines the unit vectors  $\mathbf{q}_k$  as

$$\mathbf{q}_k = U.\mathbf{v}_k = \frac{1}{\sqrt{\lambda_k}} U(S + L)\mathbf{v}_k = \frac{1}{\sqrt{\lambda_k}} R\mathbf{v}_k. \quad (2.2.11)$$

The solution to find the constraint minimum of the minimum of the proposed cost function in (2.2.1) is then given by,

Kabsch's Optimal Rotation

$$u_{ij} = \sum_k b_{kl} a_{kj}. \quad (2.2.12)$$

### **2.2.2 Examples**

There are clever ways of solving the optimal rotation between two vectors.

There is a jupyter notebook at the following link: [Kabsch Algorithm and Implementation](#). For your convenience, it is included as a pdf file below.

# Kabsch

December 15, 2020

## 0.1 Overview

Throughout this course, we will be leveraging Google's Colab Notebooks to reinforce the concepts we have been learning in class. For an introduction into how to use collab, in case you are not already familiar with it, have a go at this [overview of Colaboratory features](#).

### 0.1.1 Kabsch's Algorithm

As stated in the course notes, the Kabsch algorithm is a very versatile tool for optimally aligning two vectors to one another. In this example, we are provided with two point sets - a model set and a point (measured) set, and our goal would be to compute the optimal rotation matrix  $U$  that allows us to efficiently rotate the point set into the model set.

### 0.1.2 Load the Measured Point Set

For the example we are interested in, we have measured the position of an object in 3D space using a Northern Digital Inc's [Polaris Camera](#). The points are collected as a set of three-dimensional (3D) points in space, arranged in rows of  $(x,y,z)$  tuples and they are as given by the `measured_points_full` function below:

```
In [9]: # Here, we are importing all the libraries we will be using in these notebook
import os
import numpy as np
from os.path import join, expanduser
import scipy.linalg as LA

In [8]: def measured_points_full():
    # these are the (x,y,z) tuples
    pre_calib = {
        '0,0,0': [-369.88531494140625, 101.30087280273438, -1960.3780517578125],
        '200,0': [-369.8937683105469, 101.32111358642578, -1960.302734375],
        '0,0,1': [-369.8780212402344, 101.32646942138672, -1960.353271484375],
        '220,0': [-369.8780212402344, 101.32646942138672, -1960.353271484375],
        '0,0,2': [-367.74957275390625, 101.65080261230469, -1953.7960205078125],
        '240,0': [-370.8532409667969, 101.074951171875, -1942.255126953125],
        '0,0,3': [-366.7646484375, 101.17594909667969, -1949.628173828125],
        '255,0': [-381.33837890625, 97.10205078125, -1920.667236328125],
        '0,0,4': [-368.0609436035156, 100.83153533935547, -1953.857177734375],
        '0,220': [-382.8047790527344, 100.34918975830078, -1944.807373046875],
```

```

'0,0.5': [-369.7981262207031, 100.01362609863281, -1958.6396484375],
'0,240': [-382.71600341796875, 99.87244415283203, -1945.184326171875],
'0,0.6': [-370.24237060546875, 98.66026306152344, -1957.2281494140625],
'0,255': [-382.71600341796875, 99.87244415283203, -1945.184326171875],
'0,0.7': [-370.1295166015625, 98.33242797851562, -1956.1732177734375],
]
def exp(x):
    'This function expands the array along the second dimension so that '
    return np.expand_dims(x, 1)

# sort pre-recorded points in the order.
measured_calib = np.array([[[
    pre_calib['0,0.0'],
    pre_calib['0,220'],
    pre_calib['0,0.1'],
    pre_calib['0,240'],
    pre_calib['0,0.2'],
    pre_calib['0,255'],
    pre_calib['0,0.3'],
    pre_calib['200,0'],
    pre_calib['0,0.4'],
    pre_calib['220,0'],
    pre_calib['0,0.5'],
    pre_calib['240,0'],
    pre_calib['0,0.6'],
    pre_calib['255,0'],
    pre_calib['0,0.7'],
]]])
"""

As it is currently, our array has 3 dimensions. We need to reduce the size of the
array along the singleton dimension for efficient matrix manipulations, hence why we
are squeezing the matrix
"""

measured_calib_zero_centered = np.array(([0, 0, 0]))
for i in range(len(measured_calib)):
    ' find the centroid of the points '
    centered = measured_calib[i] - np.min(measured_calib, 0)
    measured_calib_zero_centered = np.vstack((measured_calib_zero_centered, centered))
measured_calib_zero_centered = measured_calib_zero_centered[1:]

return measured_calib_zero_centered

```

### 0.1.3 Load the model set

It now behooves us to load the model set so we can begin our Kabsch computation. For this, we have them saved in a numpy array. Therefore, we will import numpy as well as associated and needed libraries necessary for our computation.

```
In [12]: model_points = np.array([
    [-1755.87720294, 866.87898685, 283.0353811],
    [-1755.76266696, 866.8540598, 282.9782946],
    [-1758.9453555, 857.8363267, 296.13326449],
    [-1759.02853104, 865.92774874, 283.52951211],
    [-1777.42772925, 826.8692224, 293.38292356],
    [-1784.34737705, 836.7521396, 281.74652354],
    [-1777.77335781, 826.96331701, 292.88727602],
    [-1783.56649649, 836.45510137, 281.56390533],
    [-1783.53245361, 836.46510174, 281.54257437],
    [-1783.6947516, 836.55773878, 281.52364873],
    [-1783.58522171, 836.46979064, 281.55684051],
    [-1783.66230977, 836.54098015, 281.50709046],
    [-1783.52724697, 836.44927943, 281.56064662],
    [-1783.59681243, 836.52118858, 281.52347799],
    [-1783.44129296, 836.40624764, 281.5671847]
])
```

#### 0.1.4 Get the point set from the function above.

```
In [13]: point_set = measured_points_full()
```

## 0.2 Now, let us calculate the transformation as we described in our notes

```
In [23]: def Kabsch(P=None, Q=None, augment_Q=True, center=True):
    '''P and Q must be nx3. This rotation is accurate.
    Rotates points in P optimally to measured reference points in Q

    Params
    ======
    Q: Points to be rotated into
    augment_Q: Whether Q was recorded without the zero/home points embedded between su
    ...
    if not isinstance(P, np.ndarray) or not isinstance(Q, np.ndarray):
        P, Q = preproc()

    # calculate the centroids
    if center:
        'This only for computed old points'
        q0 = np.mean(Q, 1)
        p0 = np.mean(P, 1)

        Q_ctr = Q - np.expand_dims(q0, 1)
        P_ctr = P - np.expand_dims(p0, 1)
    else:
        Q_ctr, P_ctr = Q, P
```

```

# add the zero points to precomputed control points
if augment_Q:
    'This only for computed old points'
    Q_aug = np.array(([0,0,0]))
    for i in range(Q_ctr.shape[0]-1):
        Q_aug = np.append(Q_aug, np.expand_dims(Q_ctr[i+1], 0),0)
        Q_aug= np.append(Q_aug, np.expand_dims(Q_ctr[0], 0),0)
    Q_ctr = Q_aug[1:]

Hmat = P_ctr.T@Q_ctr
U, S, V = LA.svd(Hmat)
d = np.sign(np.linalg.det(V@U.T))
M = np.eye(3); M[-1][-1] =d
opt_rot = V@M@U.T
opt_trans = Q_ctr.T- opt_rot@P.T

return opt_rot, np.mean(opt_trans, 1)

```

### 0.2.1 Test the algorithm

Remember that we are rotating the points in point\_set into model\_points. So we would go ahead and call the Kabsch function above as follows:

In [24]: Rot, Trans = Kabsch(model\_points, point\_set, augment\_Q=False, center=False)

In [25]: print(Rot)

```
[[1. 0. 0.]
 [0. 1. 0.]
 [0. 0. 1.]]
```

In [26]: print(Trans)

```
[1775.85125374 -842.66314863 -284.40256961]
```

**Homework 3.** For the following model points  $P$  and measured points  $Q$ , compute the optimal rotation matrices for moving points  $Q$  into point  $P$ . For the three assignments below, report your results within a colab notebook, download the colab notebook as a pdf and upload on Latte.

1.

$$P = \begin{bmatrix} -1 & 0 & 0 \\ 0 & 0 & 0 \\ 0 & 1 & 1 \end{bmatrix}, \quad Q = \begin{bmatrix} 0 & -1 & -1 \\ 0 & -1 & 0 \\ 0 & 0 & 0 \\ -1 & 0 & 0 \end{bmatrix} \quad (2.2.13)$$

2.

$$P = \begin{bmatrix} 3172.79468418 & 727.52462347 & 7122.70450243 \\ 165.28953155 & -3552.32467068 & -2045.15346584 \\ 5292.45250241 & -1748.52037006 & -6181.40300009 \\ 1893.07584225 & 5897.19719625 & 3130.41287776 \end{bmatrix}, \quad (2.2.14)$$

$$Q = \begin{bmatrix} 1774.11606309 & -4241.11341178 & 5259.04277742 \\ 6079.70499031 & -98.14197972 & -3442.0914569 \\ 813.07069876 & 3334.26289147 & -6112.55652513 \\ 1856.72080823 & 2328.86927901 & 6322.16611888 \end{bmatrix}$$

3. For a toy problem, measure the coordinates of an object in the world using your favorite measuring instrument (a 3D camera sensor, iPhone app (e.g. ArkIt), android app e.t.c.). Be sure to record the position of the object at multiple points in world coordinates and make sure that the physical locations of these points are known (these are your model points). Then compute the optimal rotation and translation between the model and measured points.

### 2.2.3 Corresponding Point Set Registration with Quaternions

While the Kabsch algorithm does yield an optimal solution for the rotation of two sets of points that correspond to one another, it leverages the orthonormal rotation matrix with positive determinant

in its computations. This suffers from the non-uniqueness of solutions that arise from reflections. Using matrices straightforward is problematic because we need six nonlinear constraints to guarantee the orthonormality of the rotation matrix. To yield a least squares rotation, and translation, we will generally avoid singular value decomposition (SVD) methods in two and three dimensions since we generally do not want reflections. For  $n > 3$  in any  $n$ -dimensional application, the SVD approach, based on the cross-covariance matrix of two point distributions, does generalize easily to  $n$  dimensions.

Let  $\mathbf{t} = [t_x, t_y, t_z]^T$  denote the translation vector and  $\mathbf{q}_R = [q_0, q_1, q_2, q_3]^T$  denote the unit quaternion. Suppose further that the complete registration set of vectors is  $\mathbf{H} = [\mathbf{q}_R | \mathbf{t}]^T$ . Now, let  $D_l = \{\mathbf{d}_{l_i}\}$  be the measured set of points which we want to align with the model point set  $D_r = \{\mathbf{d}_{r_i}\}$ , where the cardinality,  $N_l$  of  $D_l$  is same as that of  $D_r$ ,  $N_r$ , and where each point  $\mathbf{d}_{l_i}$  corresponds to point  $\mathbf{d}_{r_i}$  with the same index. We are looking for a transformation of the form

$$D_r = a\mathbf{R}(D_l) + \mathbf{t} \quad (2.2.15)$$

from the left to the right coordinate system as shown in Fig. 4.4, where  $a$  is a scale factor, and  $\mathbf{t}$  is the translation vector offset.  $R(D_l)$  denotes the rotated version of  $D_l$ . Since we do not expect to have a perfect data, it will be difficult to find a scale factor, a translation and a rotation so that the transformation equation is satisfied for every point. Thus, there will be a residual error,

$$\mathbf{e}_i = \mathbf{d}_{r,i} - a\mathbf{R}(\mathbf{d}_{l,i}) - \mathbf{t} \quad (2.2.16)$$

and the cost function will minimize the sum of squares is given as,

$$f(\mathbf{s}) = \min \|\mathbf{e}_i\|^2. \quad (2.2.17)$$

## Finding Translation

We can find the translation, scale and finally rotation by systematically varying the total error.

Consider the centroids of the measured and point sets,

$$\bar{D}_l = \frac{1}{n} \sum_{i=1}^n \mathbf{d}_{l,i}, \quad \bar{D}_r = \frac{1}{n} \sum_{i=1}^n \mathbf{d}_{r,i}, \quad (2.2.18)$$

so that the new coordinates are

$$\mathbf{d}'_{l,i} = \mathbf{d}_{l,i} - \bar{\mathbf{d}}_l, \quad \mathbf{d}'_{r,i} = \mathbf{d}_{r,i} - \bar{\mathbf{d}}_r. \quad (2.2.19)$$

If we write  $\mathbf{t}' = \mathbf{t} - \bar{\mathbf{t}} + a\mathbf{R}(\mathbf{d}_l)$ , it follows that we can write the error as

$$\mathbf{e}_i = \mathbf{d}'_{r,i} - a\mathbf{R}(\mathbf{d}'_{l,i}) - \mathbf{t}' \quad (2.2.20)$$

and the sum of squares of errors becomes

$$\sum_{i=1}^n \|\mathbf{d}'_{r,i} - a\mathbf{R}(\mathbf{d}'_{l,i}) - \mathbf{t}'\|^2 \equiv \sum_{i=1}^n \|\mathbf{d}'_{r,i} - a\mathbf{R}(\mathbf{d}'_{l,i})\|^2 - 2\mathbf{t}' \cdot \sum_{i=1}^n [\mathbf{d}'_{r,i} - a\mathbf{R}(\mathbf{d}'_{l,i})] + n\|\mathbf{t}'\|^2. \quad (2.2.21)$$

The middle term on the right hand side vanishes since the measurements are referred to the centroid and we are left with the first and the third terms. The first term is independent of  $\mathbf{t}'$  and the last term cannot be negative given the squared norm. Thus, the total error to be minimized with  $\mathbf{t}' = 0$  is

### Optimal Translation

$$\mathbf{t} = \bar{\mathbf{d}}_r - a\mathbf{R}(\bar{\mathbf{d}}_l) \quad (2.2.22)$$

In other words, *the translation is the difference between the right centroid and the scaled and rotated left centroid.*

We can now rewrite the error term from (2.2.20) as

$$\mathbf{e}_i = \mathbf{d}'_{r,i} - a\mathbf{R}(\mathbf{d}'_{l,i}) \quad (2.2.23)$$

since  $\mathbf{t}' = 0$ . So the total error to be minimized is

$$\sum_{i=1}^n \|\mathbf{d}'_{r,i} - a\mathbf{R}(\mathbf{d}'_{l,i})\|^2. \quad (2.2.24)$$

## Finding Scale

Expanding (2.2.24), we find that

$$\sum_{i=1}^n \|\mathbf{d}'_{r,i}\|^2 - 2a \sum_{i=1}^n \mathbf{d}'_{r,i} \cdot R(\mathbf{d}'_{l,i}) + s^2 \sum_{i=1}^n \|\mathbf{d}'_{l,i}\|^2, \quad (2.2.25)$$

and since rotation preserves distances,  $\|R(\mathbf{d}'_{l,i})\|^2 = \|\mathbf{d}'_{l,i}\|^2$ , we can write the foregoing as  $S_r - 2sD + s^2S_l$ , where  $S_r$  and  $S_l$  are the sums of the squares of the measurement vectors (relative to their centroids), while  $D$  is the sum of the dot products of corresponding coordinates in the right system with the rotated coordinates in the left system. Completing the square in  $s$ , we find that

$$\left(a\sqrt{S_l} - D/\sqrt{S_l}\right)^2 + (S_r S_l - D^2)/S_l. \quad (2.2.26)$$

If we minimize with respect to scale  $a$  when the first term is 0 or  $a = D/S_l$ , we find that

$$s = \frac{\sum_{i=1}^n \mathbf{d}'_{r,i} \cdot R(\mathbf{d}'_{l,i})}{\sum_{i=1}^n \|\mathbf{d}'_{l,i}\|^2}. \quad (2.2.27)$$

## Finding rotation

To find the optimal rotation, we note that the cross-covariance matrix  $\Sigma_{lr}$  between the sets  $D_l$  and  $D_r$  is given by

$$\Sigma_{lr} = \frac{1}{N_l} \sum_{i=1}^{N_l} [(\mathbf{d}_{l,i} - \bar{\mathbf{d}}_l)(\mathbf{d}_{r,i} - \bar{\mathbf{d}}_r)^T] \quad (2.2.28)$$

$$= \frac{1}{N_l} \sum_{i=1}^{N_l} [\mathbf{d}_{l,i} \mathbf{d}_{r,i}^T] - \bar{\mathbf{d}}_l \bar{\mathbf{d}}_r^T. \quad (2.2.29)$$

The cyclic components of the skew symmetric matrix  $Q_{ij} = (\Sigma_{lr} - \Sigma_{lr}^T)_{ij}$  are used to construct the column vector  $\Delta = [Q_{23} \quad Q_{31} \quad Q_{12}]^T$ , so that the vector is then used to form the symmetric matrix

$$Q(\Sigma_{lr}) = \begin{bmatrix} \text{tr}(\Sigma_{lr}) & \Delta^T \\ \Delta & \Sigma_{lr} + \Sigma_{lr}^T - \text{tr}(\Sigma_{lr})\mathbf{I}_3 \end{bmatrix} \quad (2.2.30)$$

where  $\mathbf{I}_3$  is the  $3 \times 3$  identity matrix and the unit eigenvector  $\mathbf{q}_R = [q_0 \quad q_1 \quad q_2 \quad q_3]^T$  that corresponds to the maximum eigenvalue of  $Q(\Sigma_{lr})$  is chosen as the optimal rotation.

### 2.3 Iterative Closest Point

The Iterative Closest Point (ICP) algorithm applies to the following sets of problems (i) sets of points, (ii) sets of line segments, (iii) sets of parametric curves, (iv) sets of implicit curves, (v) sets of triangles, (vi) sets of parametric surfaces, and (vii) sets of implicit surfaces. To properly describe the algorithm, we choose a data,  $P$ , which is to be moved or registered/positioned to best align with a “model” data  $X$ . It is best if the data and model shape are decomposed into a point set if they are not already in point set form. For triangles and line segments, we use their vertices and endpoints respectively; while for curves and surfaces, an approximation to the vertices and endpoints of triangles and lines are used. Suppose we denote, as before, the number of points in the data shape as  $N_p$  and  $N_x$  as the number of points, line segments, or triangles in the model shape. The distance metric  $d$  between an individual data point  $\mathbf{p}$  and a model shape  $X$  will be denoted

$$d(\mathbf{p}, X) = \min_{\mathbf{x}(X)} \|\mathbf{x} - \mathbf{p}\|. \quad (2.3.1)$$

The closest point in  $X$  that yields the minimum distance is denoted  $\mathbf{y}$  such that  $d(\mathbf{p}, \mathbf{y}) = d(\mathbf{p}, X)$ , where  $\mathbf{y} \in X$ .

- Quiz 2.**
1. What is the worst case asymptotic computation for the closest point in  $X$  and why?
  2. What is the expected worst case computation time?

When the closest point computation from  $\mathbf{p}$  to  $X$  is performed for each point  $P$ , that process is worst case  $O(N_p N_x)$ . Let  $Y$  denote the resulting set of closest points, and  $\mathcal{C}$  the closest point operator, *i.e.*

$$Y = \mathcal{C}(P, X). \quad (2.3.2)$$

For the resultant corresponding point set  $Y$ , the least squares registration can be computed as

$$content... \quad (2.3.3)$$

## CHAPTER 3

### RIGID BODY MOTIONS: INTRODUCTION

We are chiefly concerned with *rigid bodies* and occasionally *semi-rigid* or *soft* bodies connected together by *joints*. In general, we take robots to be *mechanisms* that are made up of *links* connected to one another by *joints*. Typically, the joints connect two or more links and are formed by simple contact with adjacent bodies. Sometimes, the joints may be flexible – whether by belt, band, spring or some kind of elastic component such as bellows, diaphragms, tendons (Bern et al., 2017), fiber-reinforced elastomers (Bishop-Moser et al., 2012), resilient pads, strip, or bush. The assembly formed after the various connections between links and joints are called a *kinematic chain*.

A kinematic chain is a form of a *mechanism*. A “*mechanism can be interpreted as a means of transmitting, controlling, or constraining relative movement*” (Hunt, 1977). The term *kinematics* is generally used to describe the motion of a rigid body in space. It also applies to the motion of a semi-rigid or a completely soft robot in space. The rigid, semi-rigid or completely soft kinematic systems that allow a body to exhibit motion under a/some controlled motion of its freedom in space with respect to a fixed base frame are what we describe in this module.



Figure 3.1: Early serial kinematic chain robot manipulators. *Left:* The Stanford Arm Serial Manipulator, 1969. ©Infolab, Stanford University. *Right:* The PUMA robot arm. Reprinted from Wikipedia.

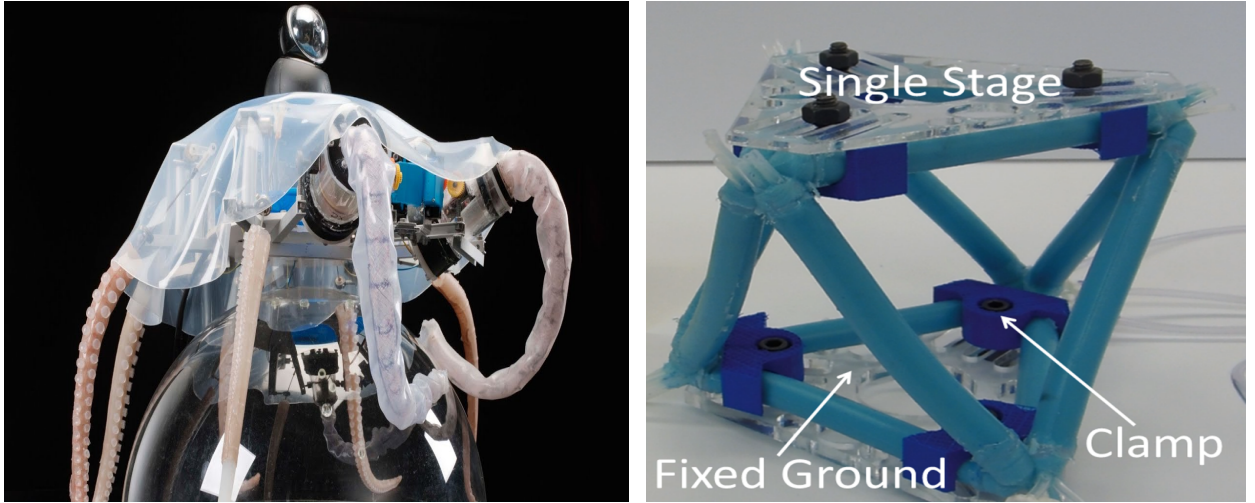


Figure 3.2: Soft Robot Manipulators *Left*: An octopus inspired soft robot. Robots classified under muscular hydrostats. ©Cecilia Laschi. *Right*: A soft parallel robot manipulator ([Hopkins et al., 2015](#)).

### 3.1 Robots Components

The joints of a robot can be *revolute* or *prismatic*. Revolute joints allow rotation about a fixed axis between two or more links while prismatic joints allow a linear motion about an *axis* – which is between two links. Symbolically, the revolute joint is denoted by  $R$  while the prismatic joint is denoted by  $P$ . By this logic, it follows that a robot made up of three links that are connected by a prismatic joint would be characterized as a *PPP* arm, while a three link arm whose links are all connected by three rotary joints would be denoted as an *RRR* arm.

A mathematical way to abstract the interconnection between the links of a robot arm is to denote the axis of rotation or the axis of translation by  $z_i$  for the joint that connects link  $i$  to link  $i + 1$ . When we characterize the robot’s motion, it often helps to work in a so-called *generalized coordinate*. Now consider a rigid body such as a link of a robot arm for example. This link contains myriads of particles, with each particle having its own position and orientation in the world. How can we describe the motion of this rod given its infinitely many particulate matter? For rigid bodies, classical mechanics comes to the rescue. As such, for a revolute joint of a rigid robot manipulator for example, the generalized coordinate is often the *joint angle*  $\theta$ , while for a prismatic joint it is the

link length  $d$  – representing the relative displacement between adjacent links. When the body we speak of is a continuum, the motion of each particle within a link needs to be accounted for. In such scenarios, researchers often work with a so-called a **Frenet-Serret** frame that models a curve on the soft robot’s surface – with or without torsion. This simplifies the dynamics and kinematics of the system and the specification of these generalized coordinates uniquely determines the position of all the particles (in a material sense for a rigid system) that make up the robot. For more examples on parameterizing soft robots, please look through some of the following references: ([Ogunmolu et al., 2015](#)), ([Hannan and Walker, 2000](#)) ([Ogunmolu et al., 2016](#)), ([Renda and Seneviratne, 2018](#)), ([Shepherd et al., 2011](#)), ([Hannan and Walker, 2003](#)), ([Ogunmolu et al., 2017](#)), ([Giorelli et al., 2015](#)), ([Ogunmolu et al., 2020](#)), ([Renda et al., 2014](#)), ([Ogunmolu, 2019a](#)), ([Ogunmolu, 2019b](#)).

### 3.2 Robot Spaces, Geometries, and Classifications

The location of a robot in the world is described by its *configuration*. This configuration specifies the positions of all points of the robot. While the coordinates of these points may be multiple over a continuous range of real numbers, the smallest number of independent variables of these real-valued coordinates needed to represent the robot configuration are the *degrees of freedom* of the system. In general, a *free rigid body* has six degrees of freedom. The motion of the robot could be about a translation or rotary axis. The  $n$ -dimensional space that contains all the possible configurations of the robot is the *configuration space* (or *C-space*) of the robot. The configuration of the robot is expressed by a point in its C-space.

A manipulator with more than 6-DOF is said to be *kinematically redundant*. The set of variables that together with a description of the manipulator’s dynamics and future inputs that determines the future transient response of the manipulator is the *state* of the robot, while the set of all possible states is referred to as the *state space*. For a rigid robot manipulator for example, the material and referential description alone is sufficient to describe the dynamics, which are Newtonian in nature. For such systems, the state may be specified by the joint variables  $\{q, \dot{q}\}$  signifying the

joint angles and joint velocities. For continuum systems, such representations are often inadequate. A popular method is to introduce a Frenet-Serret (you can read more about F-S frames in the link included earlier) frame on the body of the soft robot (SoRo) and characterize the state space based on the three parameters *i.e.*  $\{\mathcal{K}, l, \alpha\}$  that characterize the kinematic motion of the body viz., curvature of an arc projected on the SoRo's body,  $\mathcal{K}$ , the arc's length,  $l$ , and the angle subtended by a tangent along that arc,  $\alpha$ .

### 3.3 Characterization of Kinematic Geometry

As mentioned earlier, disassociated from the dynamics (*i.e.* forces, torques and such) of a body, that which deals with the displacements, or movements of a body relative to another within a mechanism is termed the *kinematics*. The displacement could be linear, angular – and in combination with the derivatives with respect to time of such displacements viz., velocities, accelerations, and hyper-accelerations all are part of the kinematics of a body. The other branch of *dynamics*, called *kinetics*, determines the forces, torques, energy, momenta, inertia, equilibrium and dynamic stability of the system and that is treated in a separate module in this course.

#### 3.3.1 Kinematic Geometries

Kinematic geometry deals only with the *displacements* of a system in the first and simplest segment of kinematics. In general, the use of time as a variable is shunned upon since the displacements we intend to carry out may be performed as fast as user wishes in their implementation. For the rest of this subsection, by kinematics, we shall mean the displacement of rigid bodies or “the solid geometry of relatively moving bodies”.

The majority of robot arms (at least today) have their actuators (or joints) connected in series along an *anthropomorphic* arm, with each joint being either at or associated with a single DOF in the robot arm. Fig. 3.3 describes the two major ways rigid links are actuated today. From a geometric point of view, both types of actuation in Fig. 3.3 serve the same purpose, which is to

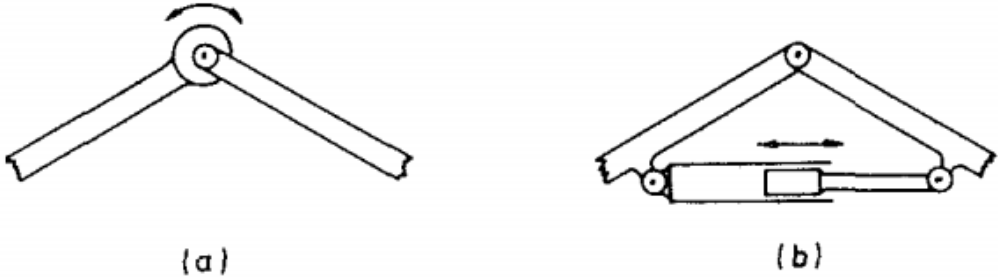


Figure 3.3: Schematic description of in-series-actuated robot arms: (a) rotary joint actuated “about” the hinge (b) prismatic joint actuated “across” a hinge. Reprinted from ([Hunt, 1983](#)).

control the rotation of the joint. However, when we are interested in controlling “pure translation” such as sliding between links, non-pivoted linear actuators are used on their own.

### 3.3.2 Open Kinematic Chains

When the links are serially connected to one another and there is no link that connects the base link to the tool frame, the robot is said to be in-series actuated. Series-jointed links have a major disadvantage, namely that they accumulate errors from shoulder out to end-effector and they suffer from a lack of rigidity. In order to eliminate their inherent load-dependent error, manufacturers typically stiffen them. However, this stiffening process increases the mass of the arm such that greater demand is placed on the actuation system. Some manufacturers employ a compensated actuation or sophisticated control techniques in order to overcome the load-dependent errors.

Examples of in-series actuated mechanisms is the *spherical robot* (see [Fig. 3.5](#)), where a succession of the robot segments are linked to the predecessors by revolute joints. By actuating each of the  $n$  joints we can control the  $n$  degrees of freedom of the end-effector. The SCARA robot, shown in [Fig. 3.5](#) is an example that allows the control of the end-effector based on the geometry of the previously connected links.

It is ideally desirable to keep the load-to-mass ratio of a robot as minimum as possible whilst preserving positioning accuracy. This is so as to preserve two important properties of the robot:



Figure 3.4: The Staubli 6-DOF Arm is an example of a Spherical Manipulator. Reprinted from DirectIndustry's Webpage.

repeatability (*i.e.* the maximum distance between two positions of the end-effector reached for the same desired pose from different starting positions), and absolute accuracy (*i.e.* distance between the desired and actual position of the end-effector) respectively. Positioning accuracy is a function of the deformation of flexure – typically not accounted for by the robot's internal sensors –



Figure 3.5: The SCARA Arm. ©Fanuc America.

and the absolute accuracy. The absolute accuracy is a function of the sensors at the manipulator joints, the clearance for the drive, flexure of links, and geometric accuracy of link orientations inter alia. When geometric constraints are violated (take a small error in the perpendicularity between successive links of a spherical arm, for example), large errors are bound to occur in the vertical motions so that such errors must be accounted for during manufacture. The conventional approach to overcoming this currently is for manufacturers to stiffen the robot's links. However, stiffening the links is tantamount to overall heavier mass, which in turn means the manipulator experiences higher inertia, centrifugal and Coriolis forces – these complicate motion planning for complex trajectories.

As we close this part of the module, bear in mind that open kinematic chains are governed by inertia and centrifugal forces – forces that exist on different scales. For example, inertia forces are a function of the square of the link lengths while frictional forces are not affected by the such dimensions. As such, serial robots cannot be scaled down to a micro level as inertia forces would be reduced while frictional forces would remain unchanged. It is not surprising that these attributes listed make serial manipulators exhibit poor positioning accuracy.

### 3.3.3 Closed-loop Kinematic Chains

When the number of links connected to a joint (the *connection degree*) is more than 2, we have a closed-loop kinematic chain. Closed-loop kinematic chains resolve the accuracy problems of open-loop chains by mechanically distributing the load on the links: they link the end-effector to the ground by a set of links that support only a fraction of the load. While theoretical works that envisioned parallel mechanisms have been in existence since 1645 (Merlet, 2015), the Stewart (Stewart, 1965) and Gough (Gough, 1957) platforms are the original designs of closed-loop chains on record. The mechanical arrangement of the links of the platform help with the load-to-mass ratio: the manipulator mass is reduced, and the disturbing effects of the Coriolis forces decreases. Albeit, these manipulators typically have a smaller workspace. Formally, we define a



Figure 3.6: Stewart-Gough Platforms *Left*: The 1954 Octahedral hexapod of the original Gough platform. *Right*: The retired platform from Dunlop tires in 2000. Picture courtesy of Parallemic.org.

*generalized parallel manipulator* as a closed-loop kinematic chain mechanism whose end-effector is linked to the base by many independent kinematic chains ([Merlet, 2015](#)).

### 3.4 Freedom and Structure in Mechanisms

Early on, we briefly defined what constitutes the degrees of freedom of a rigid body. We will now systematically analyze how to determine the mobility of a mechanism given its *kinematic pairs*, linkages and freedoms.

#### 3.4.1 Freedom, Connectivity and Mobility

For every *kinematic pair*<sup>1</sup>, there exists a characteristic number of the degrees of freedom that characterize its mobility. If a kinematic pair has elements that touch at a single point, we would have five degrees of freedoms – two of which would be translatory and three rotary. A kinematic pair whose elements always touch along a line or a curve has four or fewer degrees of freedom, or for short, freedom (see [Fig. 3.7](#)).

---

<sup>1</sup>Bonus homework: Research what is a kinematic pair and produce a one-page written report.

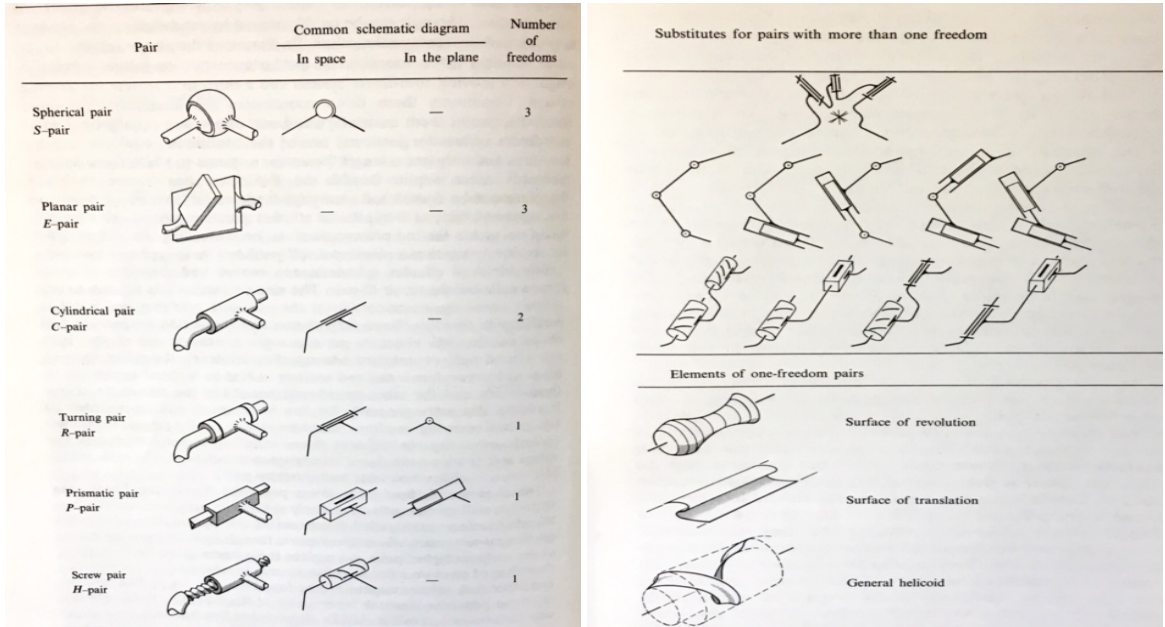


Figure 3.7: The Lower Kinematic Pairs. Reprinted from (Hunt, 1977).

However, in mechanisms, we are more concerned about the relative motion between objects in the mechanisms that do not directly touch one the other. In such systems, what we do is consider the freedom that is contributed by each of the several kinematic pairs that connect them. For the popular four bar linkage, for example (see (Murray, 1994)), the four *R*-pairs on the two connectivity-links 2 and 4 complete a *coupling* or *connection* between 1 and 3. This is said to have a connectivity of 1, typically written as  $\mathcal{C}_{13} = 1 = \mathcal{C}_{31}$ . Note that here, all connectivities are the same , and  $\mathcal{C}_{ij} = 1$ , for  $i \neq j$  and  $i, j = 1, 2, 3, 4$ . Now, suppose that the *R* pairs are replaced by spherical, or for short, *S* pairs, then we have an additional so-called *spin-freedom* about the *SS* axis (see figure Fig. 3.8) so that  $\mathcal{C}_{13} = 2$ . In any case,  $\mathcal{C}_{12} = \mathcal{C}_{13} = \mathcal{C}_{43} = 2$ .

Related to the concept of connectivity and more popular in literature is the concept of *relative mobility* or simply *mobility*. The mobility,  $\mathfrak{M}$ , is usually referred to as the number of *degrees of freedom* of a mechanism. To specify the independent variables needed to determine all the relative locations of the complete members of a mechanism with respect to one another, we typically use the *mobility criterion*. As such, we would have the kinematic chain of the left inset of Fig. 3.8 having  $\mathfrak{M} = 1$  since only an angle between the elements of any of the four kinematic pairs is

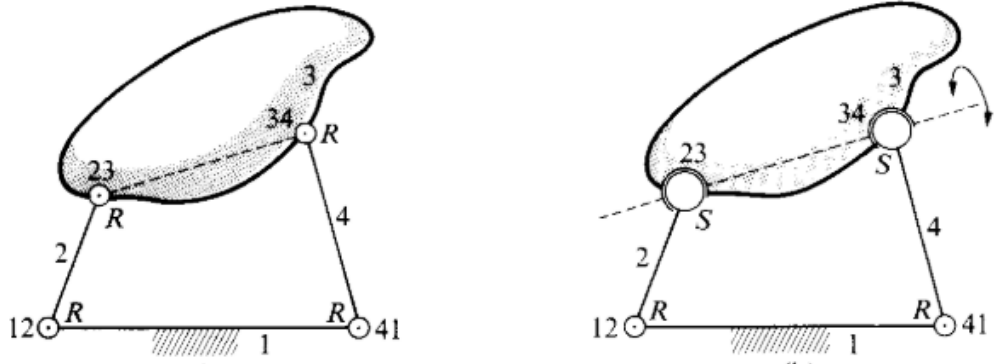


Figure 3.8: The planar  $RRR$  linkage, (left) is modified in (right) to allow spatial spin-movement of the coupler 3; the connectivity  $\mathcal{C}_{13} = 2$ ). Reprinted from (Hunt, 1977).

required so as to prevent all relative movement. However, for the  $RSSR$  mechanism on the right of Fig. 3.8, the mobility would be  $\mathfrak{M} = 2$  since member 3 has a spin-freedom.

#### Determining Degrees of Freedom

*Screw Coordinates* are better suited – from a kinematic standpoint, at any rate – to determine the general and impartial location of a rigid body.

### 3.4.2 Constraints and Freedoms

In rigid body kinematics, it is a given that the freedoms of a *free rigid body* is 6. But how is this determined? Suppose we have six homogeneous *screw coordinates* (to be introduced shortly)  $x_1, x_2, \dots, x_6$ , we find that the body is fixed when values are attached to all six of them. However, the physical constraining system to which the body is subjected is not likely to have for every constraint exactly one corresponding independent screw coordinate. For every constraint in the system, there is an influence on each of the six coordinates. For every independent constraint, a freedom of the body is suppressed so that the six independent constraint-equations  $f_i(x_1, x_2, \dots, x_6) = 0, i = 1, 2, \dots, 6$  must all be simultaneously satisfied. We define the *condition* as the constraint equation that describes a particular constraint algebraically. As the constraints are progressively relaxed, the corresponding constraint-equations are struck out one after

another, so that the body acquires one, two, . . . , degrees of freedom, until the body is completely free with no constraints or equations and we end up with six freedoms. Suppose the number of freedoms is  $f$  and the number of *unfreedoms* or constraints is  $u$ , it turns out that

$$u + f = 6. \quad (3.4.1)$$

### 3.4.3 The Mobility Criterion

For  $g$  working joints between a total of  $n$  bodies, the number of relative degrees of freedom can be identified with the relative mobility of the system of bodies, described as

$$\mathfrak{M} = 6(n - 1) - \sum_{i=1}^g u_i \quad (3.4.2)$$

where the summation term aggregates over all individual unfreedoms. Plugging (3.4.1) into (3.4.2), we have

$$\mathfrak{M} = 6(n - 1) - \sum_{i=1}^g 6 + \sum_{i=1}^g f_i \quad (3.4.3)$$

or

$$\mathfrak{M} = 6(n - g - 1) + \sum_{i=1}^g f_i. \quad (3.4.4)$$

Equation (3.4.4) is termed the general mobility criterion. It is attributed to Grübler (1908 and 1917), and independently to Kutzbatch (1929). In this module, we will generally call it the Grübler-Kutzbatch's mobility criterion. When there are independent kinematic chains within the body of concern, it is sometimes more convenient to write (3.4.4) as

$$\mathfrak{M} = \sum_{i=1}^g f_i - 6c \quad (3.4.5)$$

with  $c$  being the number of independent chains.

There are exceptions to the Grübler-Kutzbatch's mobility criterion such as when we have planar or spherical mechanisms. Take the four-bar linkage for example. There are four freedoms to the

kinematic pairs, yet patently it has a mobility of  $\mathfrak{M} = 1$ , and not  $\mathfrak{M} = -2$  as (3.4.5) would have us so determine it. This is because for planar and spherical mechanisms, the number of freedoms is not six as in *general* space, but three. Therefore, we write out the special version of (3.4.4) as

$$\mathfrak{M} = 3(n - g - 1) + \sum_{i=1}^g f_i. \quad (3.4.6)$$

This special nature of (3.4.6) arises because the joints' freedoms are not independent in planar motion, because the axes of the turning pairs are all directed parallel to one another, any prismatic pair being perpendicular to them. For spherical motions, the turning axes co-intersect at a single point.

**Homework 4.** Read up on the common kinematic arrangements in Section 1.3 of ([Spong et al., 2006](#)) and produce a 2-page single-spaced summary report. Your report must not contain diagrams but feel free to do as much analysis of the configurations of the various kinematic arrangements that are mentioned.

- Using the mobility condition, determine and explain why the SCARA robot of [Fig. 3.5](#) has the number degrees of freedom that you find.
- For the mobile manipulator we are using in this course, analyze the connectivities and freedoms of the kinematic pairs in the mechanism. In addition, determine the freedom of the overall mechanism and write out the mobility criterion.
- With the *Grübler-Kutzbach's mobility condition* that we have learned, analyze the mobility criteria of the mechanism of [Fig. 3.9](#). Hint: This mechanism is made up of two chains: chains  $A_3 B_3 B_1 A_1$  and  $A_2 B_2 B_4 A_4$ , and there is a fixed distance between the *U*-joints,  $A_2 A_3$  as well as  $A_1, A_4$ .

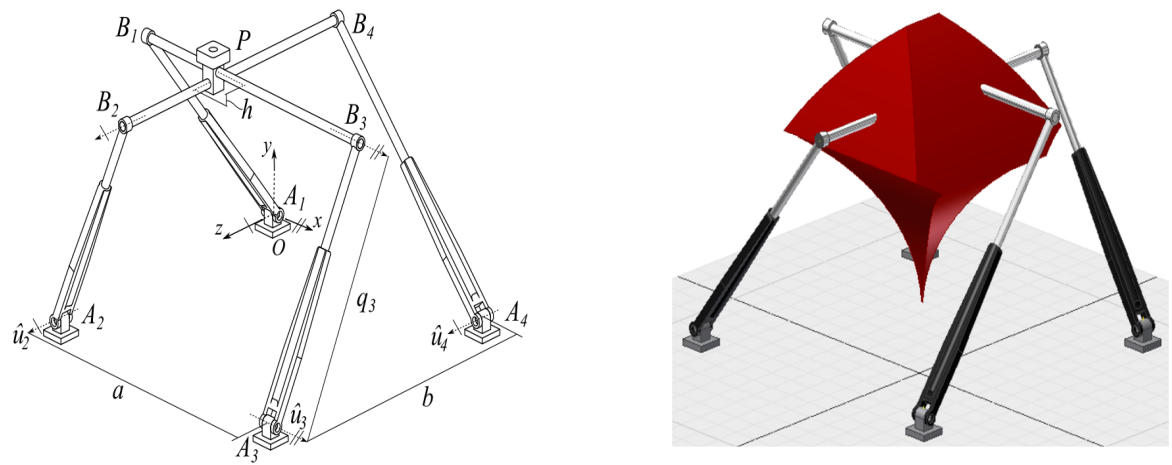


Figure 3.9: *Left:* A Parallel Planar Robot Mechanism. *Right:* Workspace of the mechanism.

## CHAPTER 4

### MOTION OF RIGID BODIES

In this chapter, we shall lay the foundations for analyzing the kinematics of a rigid or soft body in general space. Our goal is to present a geometric view of the translational and rotational rigid body motions. We take the classical screw theory approach owing to its simplicity in analyzing the geometry of kinematic motions compared against the common Denavit-Hartenberg (DH) conventions. We leave the treatment of the DH convention as an exercise for the reader. While the materials presented here may appear abstract, the applications are practical and useful. Therefore in reading the materials presented forthwith, it is recommended to the reader to ask what is it to the kinematic geometry of mechanisms that we have labored upon in [chapter 1](#). The recommended texts for this chapter are

- Murray, R. M., Li, Z., & Sastry, S. S. (1994). A Mathematical Introduction to Robotic Manipulation . Book (Vol. 29), Chapter 2
- A treatise on the theory of screws, Sir R.S. Ball, Chapter 1
- Screw theory for robotics, Jose M. Pardos-Gotors, IROS2018 tutorial; (Email the instructor for a copy).

#### 4.1 Screws

Simply put, *a screw is a line (called an axis) by which a definite linear magnitude (termed the pitch,  $p$ ) is associated*. A screw may be defined by a 6-vector of *screw coordinates*,  $\underline{s} = (S_1, S_2, S_3, S_4, S_5, S_6)$  which has the following interpretations in terms of the Plücker line coordinates of the axis

$$L = S_1, \quad M = S_2, \quad N = S_3, \quad (4.1.1a)$$

$$P = S_4 - pS_1, \quad Q = S_4 - pS_2, \quad R = S_6 - pS_3 \quad (4.1.1b)$$

where  $L, M, N$  are proportional to the direction cosines of the line forming the axis while  $P, Q, R$  are proportional to the moment of the line about the origin of the reference frame. If we scale the Plucker coordinates by  $(L^2 + M^2 + N^2)^{1/2}$ , the first three would represent the direction cosines of the line while the last three would represent the moments. We have the moment of the line as the cross product of a vector from the reference frame's origin to any point on the line with the unit vector in the line direction. Thus, we have the pitch of the screw defined as

$$p = \frac{S_1 S_4 + S_2 S_5 + S_3 S_6}{S_1^2 + S_2^2 + S_3^2} \quad (4.1.2)$$

whose magnitude is

$$\|\ell\|^2 = S_1^2 + S_2^2 + S_3^2 \quad (4.1.3)$$

for a finite pitch, otherwise, it is

$$\|\ell\|^2 = S_4^2 + S_5^2 + S_6^2 \quad (4.1.4)$$

for an infinite pitch. Note that for infinitesimal screws, scalar multiplication and vector addition are valid so that two screws,  $\underline{s}_1$  and  $\underline{s}_2$  are considered linearly dependent if there exists non-zero scalars,  $c_1$  and  $c_2$  i.e.  $c_1\underline{s}_1 + c_2\underline{s}_2 = 0$ .

#### 4.1.1 Motion screws: Twist's Pitch, Axis, and Magnitude

The unique line about which a body in space rotates or translates for an infinitesimal motion or velocity of the body is called the *twist axis*. Formally, we say *a body receives a twist about a screw when it is uniformly rotated about the screw, while it is translated uniformly parallel to the screw, through a distance equal to the product of the pitch and the circular measure of the angle of rotation* (Ball, 1908).

Similar to the screw, the *twist* is characterized by a six-vector of coordinates,  $\underline{t} = (T_1, T_2, T_3, T_4, T_5, T_6)$  so that the components of the angular velocity of the body are denoted by  $\underline{w} = (T_1, T_2, T_3)$  while

the components of the linear velocity of a fixed point in the body lying at the origin of the coordinate system is  $\underline{v} \equiv (T_4, T_5, T_6)$ .

An important thing to note is that the a twist is characterized by the attributes *pitch, magnitude and an axis*. Hence, we have the Plücker coordinates of the *twist axis* given as

**Definition 1** (Twist Axis).

$$L = T_1, \quad M = T_2, \quad N = T_3 \quad (4.1.5a)$$

$$P = T_4 - pT_1, \quad Q = T_5 - pT_2, \quad R = T_6 - pT_3. \quad (4.1.5b)$$

**Definition 2** (Pitch of a Twist). The pitch of the twist,  $\xi = \begin{pmatrix} \omega & v \end{pmatrix}^T$  is

$$p = \begin{cases} \frac{T_1 T_4 + T_2 T_5 + T_3 T_6}{T_1^2 + T_2^2 + T_3^2} = \frac{\underline{w}^T \cdot \underline{v}}{\underline{w} \cdot \underline{w}} & \text{if } \underline{\omega} \neq 0 \\ \infty & \text{otherwise} \end{cases}. \quad (4.1.6)$$

**Definition 3** (Magnitude of a Twist). The magnitude of the twist,  $\xi = \begin{pmatrix} \omega & v \end{pmatrix}^T$  is

$$\|\xi\| = \begin{cases} \|\underline{\omega}\| & \text{if } \underline{\omega} \neq 0 \\ \|\underline{v}\| & \text{otherwise} \end{cases}. \quad (4.1.7)$$

In screw theory, it is typical to concern ourselves only with the small displacements of a system's motion. Whenever a body admits an indefinitely small movement of a continuous nature, it is capable of executing that kind of movement denoted by a twist about a screw. When the body receives twists in several succession, the position that is finally attained is called the *resultant twist*.

**Homework 5.** What is the geometric meaning of (4.1.6) on a twist axis to you. Define *pure rotation* and a *pure translation* in terms of (4.1.6)<sup>1</sup>.

---

<sup>1</sup>Figure out how they correspond to zero pitch and infinite pitch twists.

### 4.1.2 Dynamics Screws: Twist's Pitch, Axis, and Magnitude

For a set of forces and moments applied to a rigid body, there is a *wrench axis*, a unique line, which has associated with it a pitch,  $p$ , and a magnitude. We may consider the set of forces and moments that act on the body to be a single force along the wrench axis and a moment about exerted about the axis. This force-moment pair is termed a *wrench*, and it is characterized by the 6-vector  $\underline{w} = (W_1, W_2, W_3, W_4, W_5, W_6)$ . We consider the first three components of  $\underline{w}$  to be the net force components,  $\underline{f}$ , exerted on the body and  $\underline{m} = \{W_4, W_5, W_6\}$  to be the components of the net moment resolved at the origin of the reference frame. We define the Plücker coordinates of the *wrench axis* as

$$L = W_1, \quad M = W_2, \quad N = W_3 \quad (4.1.8a)$$

$$P = W_4 - pW_1, \quad Q = W_5 - pW_2, \quad R = W_6 - pW_3 \quad (4.1.8b)$$

with pitch defined as

$$p = \frac{W_1W_4 + W_2W_5 + W_3W_6}{W_1^2 + W_2^2 + W_3^2} = \frac{\underline{f} \cdot \underline{m}}{\underline{f} \cdot \underline{f}}. \quad (4.1.9)$$

Equation (4.1.9) signifies that the pitch of the wrench is the ratio of the magnitude of the applied moment about a point to the magnitude of the applied force along a wrench axis. A *zero pitch wrench* would therefore correspond to pure force while an infinite pitch wrench would be a pure moment. We define the magnitude of the wrench as  $\|\underline{f}\| = \sqrt{W_1^2 + W_2^2 + W_3^2}$  when we have a finite pitch. If the pitch is infinite, the magnitude is  $\|\underline{m}\| = \sqrt{W_4^2 + W_5^2 + W_6^2}$ .

**Homework 6.** A unit screw, twist or wrench is one where the magnitude of the screw, twist or wrench is 1.

(1). What is the geometric meaning of a unit screw to you? (2) Consult the identified reference materials and explain what a reciprocal screw is in no more than five sentences.

### 4.1.3 Screw Motions

A *screw motion* is a rotation about the axis,  $l$  by an amount  $\alpha = \ell$  followed by a translation by an amount  $h\alpha$  that is parallel to the axis  $l$ . A pure translation occurs when  $h = \infty$  so that the screw motion is composed of a *pure translation* along the axis of the screw by a distance  $\ell$ .

## 4.2 Rodrigues' Formula

The matrix exponential

$$e^{\hat{\omega}t} = I + \hat{\omega}t + \frac{(\hat{\omega}t)^2}{2!} + \frac{(\hat{\omega}t)^3}{3!} + \dots \quad (4.2.1)$$

is instrumental in defining the rotation about an axis,  $\omega$ :

$$R(\omega, \theta) = e^{\hat{\omega}\theta}. \quad (4.2.2)$$

Thus, for a matrix  $\hat{\omega}$  in the Lie algebra  $so(3)$ , a unit vector  $\|\omega\| = 1$ , and a real number  $\theta \in \mathbb{R}$ , we write the exponential of  $\hat{\omega}\theta$  as

$$e^{\hat{\omega}\theta} = I + \theta\hat{\omega} + \frac{\theta^2}{2!}\hat{\omega}^2 + \frac{\theta^3}{3!}\hat{\omega}^3 + \dots \quad (4.2.3)$$

**Homework 7.** Given a matrix  $\hat{m} \in so(3)$ , suppose that the following relation holds,

$$\hat{m}^2 = mm^T - \|m\|^2 I \quad (4.2.4)$$

$$\hat{m}^3 = -\|m\|^2 \hat{m} \quad (4.2.5)$$

with the fact that higher powers of  $\hat{m}$  can be recursively found. Therefore, utilizing this lemma with  $m = \omega\theta$ ,  $\|\omega\| = 1$ , show that

$$e^{\hat{\omega}\theta} = I + \hat{\omega} \sin \theta + \hat{\omega}^2 (1 - \cos \theta). \quad (4.2.6)$$

Equation (4.2.6) is *Rodrigues' formula*.

### 4.3 The Matrix Exponential, The Lie Group and Lie Algebra

For any matrix

$$g = \begin{bmatrix} R & d \\ 0 & 1 \end{bmatrix} \in SE(3) \text{ such that } R \in SO(3), d \in \mathbb{R}^3, \text{ and } RR^T = I \quad (4.3.1)$$

there exists a matrix

$$N = \begin{bmatrix} S & x \\ 0 & o \end{bmatrix} \text{ such that } S = -S^T \quad (4.3.2)$$

such that  $\exp(N) = g$  since we can write

$$\begin{bmatrix} R & d \\ 0 & 1 \end{bmatrix} = \begin{bmatrix} I & d \\ 0 & 1 \end{bmatrix} \begin{bmatrix} R & 0 \\ 0 & 1 \end{bmatrix} = \begin{bmatrix} I & d \\ 0 & 1 \end{bmatrix} \exp \begin{bmatrix} S & 0 \\ 0 & 0 \end{bmatrix}. \quad (4.3.3)$$

We see that the exponential map is surjective onto  $\mathbb{E}(3)$ .  $SE(3)$  is Lie Group whose isomorphism is the *lie algebra*  $\mathfrak{se}(3)$ . Generally, we define the Lie Group  $SE(n)$  on the configuration of a rigid body that consists of the pair  $(p_{ij}, R_{ij})$  to be the product space of  $\mathbb{R}^n$  with  $SO(n)$ , called the **special Euclidean group** i.e.

$$SE(n) = \{(p, R) : p \in \mathbb{R}^n, R \in SO(n)\} = \mathbb{R}^n \times SO(n) \quad (4.3.4)$$

An element of  $\mathfrak{se}(3)$ <sup>2</sup> is the *twist* earlier introduced, which is the infinitesimal generator of the Euclidean group. Formally, we define  $\xi = (\omega, v) \in \mathbb{R}^6$  as the twist coordinates of  $\hat{\xi}$ . Equation (4.3.3) is basically a re-statement of *Euler's theorem, that is that a rigid body transformation is basically a rotation about a line passing through a preassigned fixed point*. Note that  $S$  is the anti-symmetric matrix or skew-symmetric matrix with the following special property

$$S(\vec{\omega}) = \hat{\omega} = \begin{pmatrix} 0 & -\omega_z & \omega_y \\ \omega_z & 0 & -\omega_x \\ -\omega_y & \omega_x & 0 \end{pmatrix} \quad (4.3.5)$$

---

<sup>2</sup>We typically write the Lie algebra in lowercase with the math frak style.

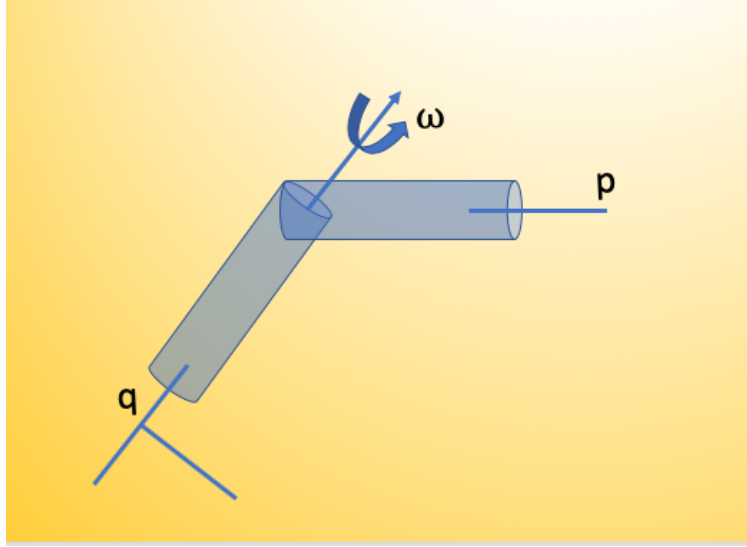


Figure 4.1: Illustration of rotation of interconnecting link of two spherical links.

that is  $\omega_x, \omega_y, \omega_z$  are the component of the vector  $\vec{\omega}$  such that

$$s_{ij} = \begin{cases} 0, & \text{if } i = j \\ -s_{ji} & \text{if } i \neq j. \end{cases}$$

It is a common convention in robotics texts to denote the skew symmetric matrix by  $\hat{\omega}$  and we will adopt that convention for the rest of these notes. In particular, we define the *homogeneous coordinates* for a point  $q \in \mathbb{R}^3$  that is rotating about an axis  $\vec{\omega} \in \mathbb{R}^3$  such that  $\|\vec{\omega}\| = 1$  (see Fig. 4.1) as

$$\hat{\xi} = g^{-1}\dot{g} = \begin{pmatrix} \hat{\omega} & v \\ 0 & 0 \end{pmatrix} \in \mathfrak{se}(3) \quad (4.3.6)$$

where  $v = -\omega \times q$ . Equation (4.3.6) is the object's velocity in the body frame; essentially the *Lie algebra element* and we can obtain the twist coordinates from it via the so-called *wedge operator*

$$\begin{pmatrix} \hat{\omega} \\ v \end{pmatrix}^\wedge = \begin{pmatrix} \hat{\omega} & v \\ 0 & 0 \end{pmatrix}. \quad (4.3.7)$$

If the link of Fig. 4.1 moves at a unit velocity, we can write the velocity at the tip point as

$$\dot{p} = \omega \times (p(t) - q(t)) \quad (4.3.8)$$

where  $p(t), q(t)$  are the paths traced out by points  $p$  and  $q$  respectively during the motion.

We define the exponential for the matrix  $A \in SO(n)$ , which is a component of the solution to the ordinary differential equation,  $\dot{x}(t) = Ax(t)$  where  $x(t) \in \mathbb{R}^n$  as

### The Matrix Exponential

$$e^{At} = I + At + \frac{A^2 t^2}{2!} + \frac{A^3 t^3}{3!} + \dots \quad (4.3.9)$$

For the matrix exponential of (4.3.9), we would like to write the equation in a closed-form expression since we are interested in definite solutions for our forward kinematics problems. For suppose that some matrix  $D \in \mathbb{R}^{n \times n}$  and  $P \in \mathbb{R}^{n \times n}$  are available, then we find that

$$\begin{aligned} e^{At} &= I + (PDP^{-1})t + (PDP^{-1})(PDP^{-1})\frac{t^2}{2!} + \dots \\ &= P \left( IDt + \frac{(Dt)^2}{2!} + \dots \right) P^{-1} \end{aligned} \quad (4.3.10)$$

$$= Pe^{Dt}P^{-1}. \quad (4.3.11)$$

**Definition 4** (Exponential Map Properties). We note the following properties of the matrix exponential:

- (1)  $d(e^{At}) = Ae^{At} = e^{At}A$ .
- (2) For  $A = PDP^{-1}$  for some diagonal  $D \in \mathbb{R}^{n \times n}$  and an invertible  $P \in \mathbb{R}^{n \times n}$ ,  $e^{At} = Pe^{Dt}P^{-1}$ .
- (3) For  $AB = BA$ , we have  $e^A e^B = e^{A+B}$ .
- (4)  $(e^A)^{-1} = e^{-A}$

For the mapping from the twist map in the Lie algebra to the Lie group notation, we have the following:

Exponential map from  $\mathfrak{se}(3)$  to  $SE(3)$

$$e^{\hat{\xi}\theta} = \begin{pmatrix} e^{\hat{\omega}\theta} & (I - e^{\hat{\omega}\theta})(w \times v) + \omega\omega^T v\theta \\ 0 & I \end{pmatrix} \in SE(3) \quad (4.3.12)$$

### 4.3.1 The Lie Group Notations

## LIE GROUP NOTATIONS

position – orientation	standard representation $\mathbf{g} = \begin{pmatrix} \mathbf{R} & \mathbf{u} \\ 0 & 1 \end{pmatrix} \in SE(3)$	Adjoint and coAdjoint representation $Ad_{\mathbf{g}} = \begin{pmatrix} \mathbf{R} & 0 \\ \tilde{\mathbf{u}}\mathbf{R} & \mathbf{R} \end{pmatrix}, Ad_{\mathbf{g}}^* = \begin{pmatrix} \mathbf{R} & \tilde{\mathbf{u}}\mathbf{R} \\ 0 & \mathbf{R} \end{pmatrix} \in \mathbb{R}^{6 \times 6}$
velocity (body frame)	Lie Algebra element $\mathbf{g}^{-1}\dot{\mathbf{g}} = \hat{\boldsymbol{\eta}} = \begin{pmatrix} \tilde{\mathbf{w}} & \mathbf{v} \\ 0 & 0 \end{pmatrix} \in \mathfrak{se}(3)$	adjoint and coadjoint map
	twist vector $\boldsymbol{\eta} = \begin{bmatrix} \mathbf{w} \\ \mathbf{v} \end{bmatrix} \in \mathbb{R}^6$	$ad_{\boldsymbol{\eta}} = \begin{pmatrix} \tilde{\mathbf{w}} & 0 \\ \tilde{\mathbf{v}} & \tilde{\mathbf{w}} \end{pmatrix}, ad_{\boldsymbol{\eta}}^* = \begin{pmatrix} \tilde{\mathbf{w}} & \tilde{\mathbf{v}} \\ 0 & \tilde{\mathbf{w}} \end{pmatrix} \in \mathbb{R}^{6 \times 6}$ Where $\tilde{\mathbf{a}} = \begin{pmatrix} 0 & -z & y \\ z & 0 & -x \\ -y & x & 0 \end{pmatrix}$
strain (body frame)	Lie Algebra element $\mathbf{g}^{-1}\dot{\mathbf{g}}' = \hat{\boldsymbol{\xi}} = \begin{pmatrix} \tilde{\mathbf{k}} & \mathbf{p} \\ 0 & 0 \end{pmatrix} \in \mathfrak{se}(3)$	adjoint and coadjoint map
	twist vector $\boldsymbol{\xi} = \begin{bmatrix} \mathbf{k} \\ \mathbf{p} \end{bmatrix} \in \mathbb{R}^6$	$ad_{\boldsymbol{\xi}} = \begin{pmatrix} \tilde{\mathbf{k}} & 0 \\ \tilde{\mathbf{p}} & \tilde{\mathbf{k}} \end{pmatrix}, ad_{\boldsymbol{\xi}}^* = \begin{pmatrix} \tilde{\mathbf{k}} & \tilde{\mathbf{p}} \\ 0 & \tilde{\mathbf{k}} \end{pmatrix} \in \mathbb{R}^{6 \times 6}$



• J. M. Selig. *Geometric Fundamentals of Robotics*. Monographs in Computer Science. Springer New York, 2007.



Figure 4.2: Lie Group and their Notations. Reprinted with permission from Federico Renda. IROS 2018, Screw Theory Tutorial.

### 4.3.2 Exponential Map and Kinematic Chains

Now consider a robot manipulator of the form shown in Fig. 3.4. The reader may imagine that there are right-handed triads of orthogonal vectors at the tip of each link of the chain so that the Euclidean transformation that describes the position and orientation of the  $(i + 1)'th$  link with the  $i'th$  link is

$$\begin{pmatrix} R_i & d_i \\ 0 & 1 \end{pmatrix} \exp \begin{pmatrix} S_i & 0 \\ 0 & 0 \end{pmatrix} \theta_i = g_i \exp(\hat{\omega}_i \theta_i) \quad (4.3.13)$$

and we may imagine the triad that is fixed at the end-effector to be related to the triad at the base of the robot by the following relation

$$H(\theta_1, \theta_2, \dots, \theta_n) = R_1 e^{\theta_1 \hat{\omega}_1} R_2 e^{\theta_2 \hat{\omega}_2} \dots, R_n e^{\theta_n \hat{\omega}_n} \quad (4.3.14)$$

and since  $P \exp(M) P^{-1} = \exp(P M P^{-1})$ , we can write the *forward kinematic map*,  $g_{st} : Q \rightarrow SE(3)$  as

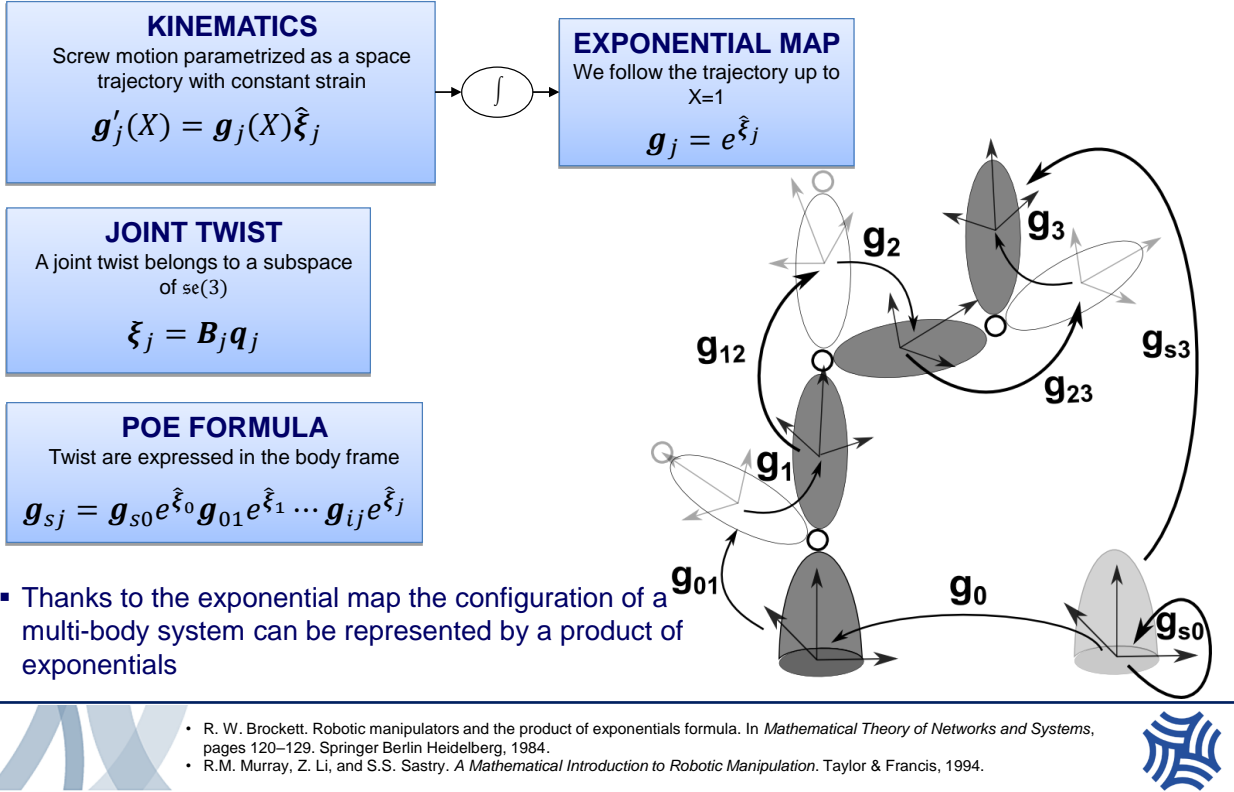
$$g_{st}(\theta) = e^{\theta_1 \hat{\omega}_1} e^{\theta_2 \hat{\omega}_2} \dots, e^{\theta_n \hat{\omega}_n} g_{st}(0) \quad (4.3.15)$$

using the identity repeatedly.

### 4.4 Rigid Body Transformations

A rigid body motion is one that preserves the distance between points. In classical mechanics, we are concerned about the material description of a rigid body whereby we consider all the particles that make up the rigid body as a whole rather than treat them as a continuum as it is typical in continuum mechanics. Therefore by this logic, *a rigid body is a collection of particles by which the distance between any two particles remain fixed, irrespective of the motions of the body or forces exerted on that body* ([Murray, 1994](#)).

# BROCKETT'S PRODUCT OF EXPONENTIALS FORMULA



• R. W. Brockett. Robotic manipulators and the product of exponentials formula. In *Mathematical Theory of Networks and Systems*, pages 120–129. Springer Berlin Heidelberg, 1984.  
• R.M. Murray, Z. Li, and S.S. Sastry. *A Mathematical Introduction to Robotic Manipulation*. Taylor & Francis, 1994.



Figure 4.3: An illustration of the exponential map for a multi-body rigid system. Reprinted with permission from Federico Renda. IROS 2018, Screw Theory Tutorial.

Suppose we have two points  $a$  and  $b$  on a rigid body, we must have

$$\|a(t_f) - b(t_f)\| = \|a(t_i) - b(t_i)\| \quad (4.4.1)$$

where  $t_i$  and  $t_f$  are two instants of time that the two points *i.e.*  $a$  and  $b$  are observed on the rigid body. We thus see that distance is preserved irrespective of observer placement in rigid body transformations. For continuum-based systems such as soft robots, this is not so and we often need to come up with clever mechanisms of characterizing the motion of its particles.

**Definition:** A mapping  $g : \mathbb{R}^3 \rightarrow \mathbb{R}^3$  is a *rigid body transformation* if it satisfies the following properties:

- Length is preserved *i.e.*  $\|g(a) - g(b)\| = \|a - b\|$  for all point  $a, b \in \mathbb{R}^3$ .
- The cross product for all vectors is preserved *i.e.*  $g(p \times q) = g(p) \times g(q)$  where  $p, q \in \mathbb{R}^3$ .

This means that the inner product is preserved so that we have,

$$p^T q = g(p)^T \times g(q). \quad (4.4.2)$$

It follows that orthogonal vectors are transformed to orthogonal vectors and since cross product is naturally preserved, rigid body transformations map orthonormal coordinate frames to orthonormal coordinate frames. Note that it is possible to have rotation of particles despite the two strong forms presented above. To track the location of a rigid body in space, it therefore follows that we need to keep track of the motion of any one point as well as the rotation of the rigid body about this point. Therefore, the *configuration* of the rigid body is found by attaching a Cartesian coordinate frame to a point on the rigid body and keeping track of the motion of the body coordinate frame with respect to a fixed frame. To ease representation, we typically require that all coordinate frames be *right-handed*: given three Cartesian orthonormal vectors  $x, y, z \in \mathbb{R}^3$  which characterize the motion of a coordinate frame, they must satisfy  $z = x \times y$ .

Going by the definitions of twist in the foregoing, it follows that a twist is to a rigid body what a vector is to a point. They both express the relation needed to transfer an object from one given position to another. When a body twists at an instant, the screw about which it twists is referred to as the *instantaneous screw*.

#### 4.4.1 Translation in $\mathbb{R}^3$

For the two coordinate frames shown in Fig. 4.4, say we choose the  $o_0x_0y_0$  frame as the reference and the  $o_1x_1y_1$  as the moving coordinate frame, the way we would characterize the translation motion of the the point  $q$  would be to represent its translation from the reference frame by the Cartesian displacement along  $x$  and  $y$  so that we have

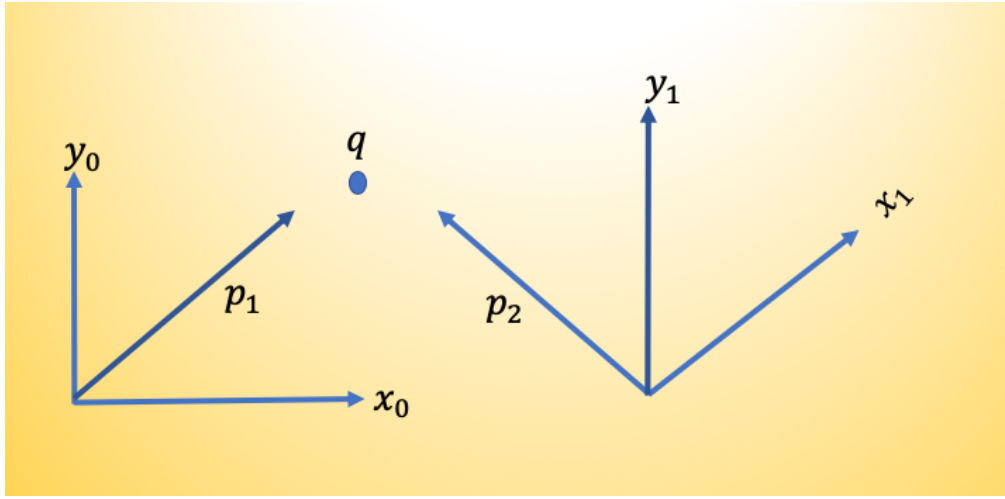


Figure 4.4: A point  $q$  in space with respect to two coordinate frames.

$$q^0 = \begin{pmatrix} q_x^0 \\ q_y^0 \end{pmatrix}, \quad q^1 = \begin{pmatrix} q_x^1 \\ q_y^1 \end{pmatrix} \quad (4.4.3)$$

where the superscript denotes the reference frame and the subscript denotes the coordinate of the point  $q$  along an axis in either Cartesian frame. The origin of the two frames are both points in space; therefore, we can assign the coordinates that denote the position of the origin of one coordinate frame with respect to another as

$$o_1^0 = \begin{pmatrix} o_x^0 \\ o_y^0 \end{pmatrix}, \quad o_0^1 = \begin{pmatrix} o_x^1 \\ o_y^1 \end{pmatrix}. \quad (4.4.4)$$

For vectors such as twists or wrenches, we use a similar notation as those used for points. Thus if  $p_1, p_2$  are two vectors that are invariant with respect to the choice of coordinate frames, we would have

$$p_1^0 = \begin{pmatrix} o_x^0 \\ o_y^0 \end{pmatrix}^T, \quad p_1^1 = R(-\theta)q^0, \quad p_2^0 = R(\theta)q^0, \quad p_2^1 = \begin{pmatrix} o_x^1 \\ o_y^1 \end{pmatrix}^T \quad (4.4.5)$$

where  $\theta$  is the angle that coordinate frame 1 makes with respect to coordinate frame 0. In robotics, the standard way to apply a rotation is counterclockwise. This is the reason we negate the angle

of rotation when finding the vector  $p_1$  in frame 1. We will introduce the definition of the rotation matrix  $R$  shortly. Performing frame transformations is a fundamental step to getting a robot work as envisioned. We must ensure that all coordinate vectors are defined with respect to the same coordinate frame. We say two vectors are “equal” when they have the same magnitude and direction. Therefore, for vectors that are not constrained to be located at the same point in space, we require that they defined with respect to frames whose coordinates are parallel, given that absolute locations are not consequential, but the magnitude and direction of the vector.

#### 4.4.2 Rotations in $\mathbb{R}^3$

We would like to establish a convention that all coordinate frames will be right-handed. Our goal is to establish the orientation of an object by specifying the local coordinate on the body; we then describe the body’s *relative orientation* between a coordinate frame attached to the body and a fixed or an inertial coordinate frame. Suppose that we have two frames  $I$  and  $J$ , where  $I$  is the inertial frame, while  $J$  is the body frame as shown in Fig. 4.5. Let  $\mathbf{x}_{ij}, \mathbf{y}_{ij}, \mathbf{z}_{ij} \in \mathbb{R}^3$  be the coordinates of the principal axes of  $J$  relative to  $I$  so that we have the following matrix as a result of composing the respective coordinate vectors

$$R_{ij} = [\mathbf{x}_{ij} \quad \mathbf{y}_{ij} \quad \mathbf{z}_{ij}] = \begin{bmatrix} r_{11} & r_{12} & r_{13} \\ r_{21} & r_{22} & r_{23} \\ r_{31} & r_{32} & r_{33} \end{bmatrix}. \quad (4.4.6)$$

The resulting matrix in (4.4.6) is the *rotation matrix*. This matrix can be rewritten by noting that the components of a vector are the projections of that vector onto the unit directions of its reference frame. Thus, the components if  $R_{ij}$  in (4.4.6) can be written as the dot product of a pair of unit vectors:

$$R_{ij} = \begin{bmatrix} \mathbf{x}_j \cdot \mathbf{x}_i & \mathbf{y}_j \cdot \mathbf{x}_i & \mathbf{z}_j \cdot \mathbf{x}_i \\ \mathbf{x}_j \cdot \mathbf{y}_i & \mathbf{y}_j \cdot \mathbf{y}_i & \mathbf{z}_j \cdot \mathbf{y}_i \\ \mathbf{x}_j \cdot \mathbf{z}_i & \mathbf{y}_j \cdot \mathbf{z}_i & \mathbf{z}_j \cdot \mathbf{z}_i \end{bmatrix}. \quad (4.4.7)$$

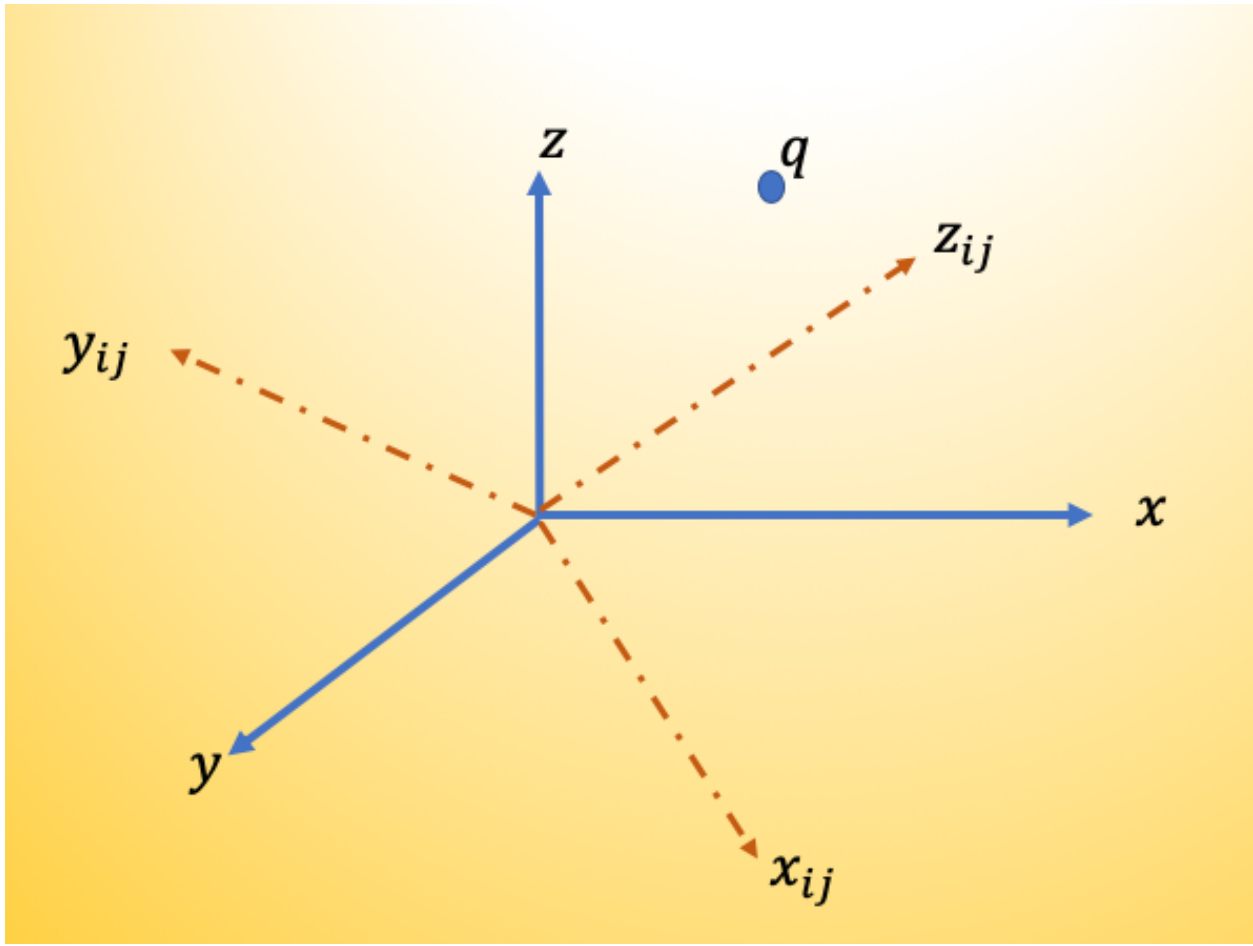


Figure 4.5: An illustration of the relative orientation of a rigid object  $q$  between an inertial frame  $I$  and a body frame  $J$ .

The components of the rotation matrix (4.4.6) are sometimes called direction cosines since the dot product of two unit vectors give the cosine of the angle between them as shown in (4.4.7). If we examine the rows of (4.4.7), we see that the rows of  $R_{ij}$  are the unit vectors coordinates of  $I$  in the frame  $J$  so that we have

$$R_{ij} = R_{ji}^T \quad (4.4.8)$$

which is to say that the inverse of the rotation matrix is equal to its transpose. Noting that  $\|\mathbf{r}\|^2 = x_i^2 + y_i^2 + z_i^2 = 1$ ,  $r_i \cdot r_j = 0$  when  $i \neq j$ , and  $r_i \cdot r_i = 0$ , this can be thus verified as

$$R_{ij}^T \cdot R_{ji} = \begin{bmatrix} \mathbf{x}_j \cdot \mathbf{x}_i & \mathbf{x}_j \cdot \mathbf{y}_i & \mathbf{x}_j \cdot \mathbf{z}_i \\ \mathbf{y}_j \cdot \mathbf{x}_i & \mathbf{y}_j \cdot \mathbf{y}_i & \mathbf{y}_j \cdot \mathbf{z}_i \\ \mathbf{z}_j \cdot \mathbf{x}_i & \mathbf{z}_j \cdot \mathbf{y}_i & \mathbf{z}_j \cdot \mathbf{z}_i \end{bmatrix} \cdot \begin{bmatrix} \mathbf{x}_j \cdot \mathbf{x}_i & \mathbf{y}_j \cdot \mathbf{x}_i & \mathbf{z}_j \cdot \mathbf{x}_i \\ \mathbf{x}_j \cdot \mathbf{y}_i & \mathbf{y}_j \cdot \mathbf{y}_i & \mathbf{z}_j \cdot \mathbf{y}_i \\ \mathbf{x}_j \cdot \mathbf{z}_i & \mathbf{y}_j \cdot \mathbf{z}_i & \mathbf{z}_j \cdot \mathbf{z}_i \end{bmatrix} \quad (4.4.9)$$

$$= \begin{bmatrix} \mathbf{x}_j \cdot \mathbf{x}_j \cdot \|\mathbf{r}\|^2 & \mathbf{x}_j \cdot \mathbf{y}_j \cdot \|\mathbf{r}\|^2 & \mathbf{x}_j \cdot \mathbf{z}_j \cdot \|\mathbf{r}\|^2 \\ \mathbf{y}_j \cdot \mathbf{x}_j \cdot \|\mathbf{r}\|^2 & \mathbf{y}_j \cdot \mathbf{y}_j \cdot \|\mathbf{r}\|^2 & \mathbf{y}_j \cdot \mathbf{z}_j \cdot \|\mathbf{r}\|^2 \\ \mathbf{z}_j \cdot \mathbf{x}_j \cdot \|\mathbf{r}\|^2 & \mathbf{z}_j \cdot \mathbf{y}_j \cdot \|\mathbf{r}\|^2 & \mathbf{z}_j \cdot \mathbf{z}_j \cdot \|\mathbf{r}\|^2 \end{bmatrix} = \begin{pmatrix} 1 & 0 & 0 \\ 0 & 1 & 0 \\ 0 & 0 & 1 \end{pmatrix} \quad (4.4.10)$$

$$= \mathbf{I}_3 \quad (4.4.11)$$

where  $\mathbf{I}_3$  is the  $3 \times 3$  identity matrix.

**Homework 8.** Verify that  $R_{ij} = R_{ji}^{-1} \equiv R_{ji}^T$ . Furthermore, verify that the determinant of the rotation matrix is  $\pm 1$  i.e.  $\det R = \pm 1$ .

The determinant of the  $R$  matrix is written as

$$\det R = r_1^T (r_2 \times r_3). \quad (4.4.12)$$

For right-handed coordinate frames, we have that  $r_2 \times r_3 = r_1$  so that  $r_1^T r_1 = 1$  for a coordinate frame that aligns with the right-hand orthonormal frame representation. This special property that a  $3 \times 3$  matrix satisfies  $r_2 \times r_3 = r_1$  and that  $\det R = r_1^T r_1 = 1$  is called the special orthogonal property, denoted  $SO(3)$ . Special orthogonal means  $\det R = +1$ . The set of all SO matrices in  $\mathbb{R}^{n \times n}$  is defined by

$$SO(n) = \{R \in \mathbb{R}^{n \times n} : RR^T = \mathbf{I}, \det R = +1\}. \quad (4.4.13)$$

#### 4.4.3 Rotation Matrices as Transformations

Suppose we are tasked with transforming a point  $q$  from one coordinate frame  $J$  to a frame  $I$  based on Fig. 4.5. Suppose that  $q_j = (x_j, y_j, z_j)$  are the coordinates of  $q$  with respect to the frame  $J$ . We

may reason that  $x_j, y_j, z_j \in \mathbb{R}^3$  are the projections of  $q$  onto the coordinate axes of  $B$ , which in turn, have coordinates  $\mathbf{x}_{ij}, \mathbf{y}_{ij}, \mathbf{z}_{ij} \in \mathbb{R}^3$  with respect to coordinate frame  $I$ ; then it follows that the coordinates of  $q$  relative to frame  $I$  is

$$q_i = \mathbf{x}_{ij}x_j + \mathbf{y}_{ij}y_j + \mathbf{z}_{ij}z_j. \quad (4.4.14)$$

which in vectorized form is

$$q_i = \begin{pmatrix} \mathbf{x}_{ij} & \mathbf{y}_{ij} & \mathbf{z}_{ij} \end{pmatrix} \begin{pmatrix} x_j \\ y_j \\ z_j \end{pmatrix} = R_{ij}q_j \quad (4.4.15)$$

where the last part of the above equation follows from (4.4.7).

Just as a rotation matrix can act on points to transform them in the world, so can rotation matrices act on vectors. Say we have another point  $p_j$  on the frame  $J$  in Fig. 4.5, then the vector that connects a point  $q_j$  in the frame  $J$  to  $p_j$  is  $v_j = q_j - p_j$  so that the action of the rotation matrix on  $v_j$  is

$$R_{ij}(v_j) := R_{ij}q_j - R_{ij}p_j = q_i - p_i = v_i. \quad (4.4.16)$$

#### 4.4.4 Planar Rotations

We now revisit the relative orientation between two coordinate frames as shown in Fig. 4.5. Suppose now that the angle of rotation between the two coordinate frames is  $\theta$  as shown in Fig. 4.6, it follows that the composition of the rotation allows us to write

$$R_1^0 = \begin{pmatrix} x_1^0 & y_1^0 \end{pmatrix} \quad (4.4.17)$$

whereupon  $x_1^0$  and  $y_1^0$  have the usual meanings as before and are expressed as

$$x_1^0 = \begin{pmatrix} \cos \alpha \\ \sin \alpha \end{pmatrix} \text{ and } y_1^0 = \begin{pmatrix} -\sin \alpha \\ \cos \alpha \end{pmatrix} \quad (4.4.18)$$

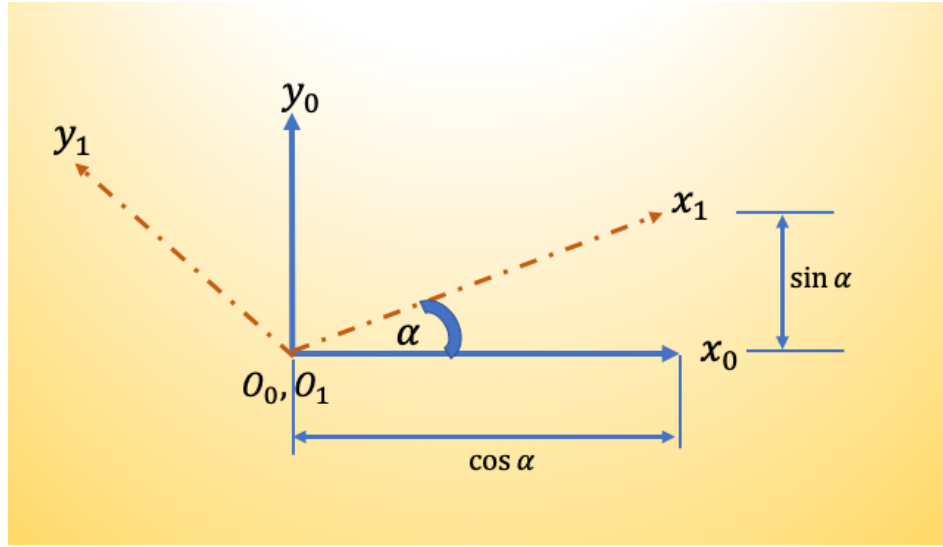


Figure 4.6: Illustration of rotation between two frames in a plane.

so that composing the rotation matrix, we have

$$R = \begin{pmatrix} \cos \alpha & -\sin \alpha \\ \sin \alpha & \cos \alpha \end{pmatrix} \quad (4.4.19)$$

While you might find the above approach rather daunting, an easier geometric way to visualize the transformation of matrices is to recall that the columns of the rotation matrix are the direction cosines of the coordinate axes of  $o_1x_1y_1$  relative to the coordinates of  $o_0x_0y_0$  c.f. (4.4.7). For a planar rotation, we could extract the first  $2 \times 2$  block of (4.4.7) so that

$$R_1^0 = \begin{bmatrix} x_0 \cdot x_1 & y_1 \cdot x_0 \\ x_0 \cdot y_1 & y_1 \cdot y_0 \end{bmatrix} \quad (4.4.20)$$

And since the dot product of two vectors is basically the cosine of the angles between them, we have

$$R_1^0 = \begin{bmatrix} \cos \alpha & -\cos(\pi/2 - \alpha) \\ \cos(\pi/2 - \alpha) & \cos \alpha \end{bmatrix} = \begin{bmatrix} \cos \alpha & -\sin \alpha \\ \sin \alpha & \cos \alpha \end{bmatrix} \quad (4.4.21)$$

Note the way the negative signs have entered the matrix due to the counterclockwise direction of rotation that we have chosen so as to preserve the positiveness of the determinant of  $R$ . In particular, the projection of  $y_1$  on  $x_0$  is negative because of our right-handed frame.

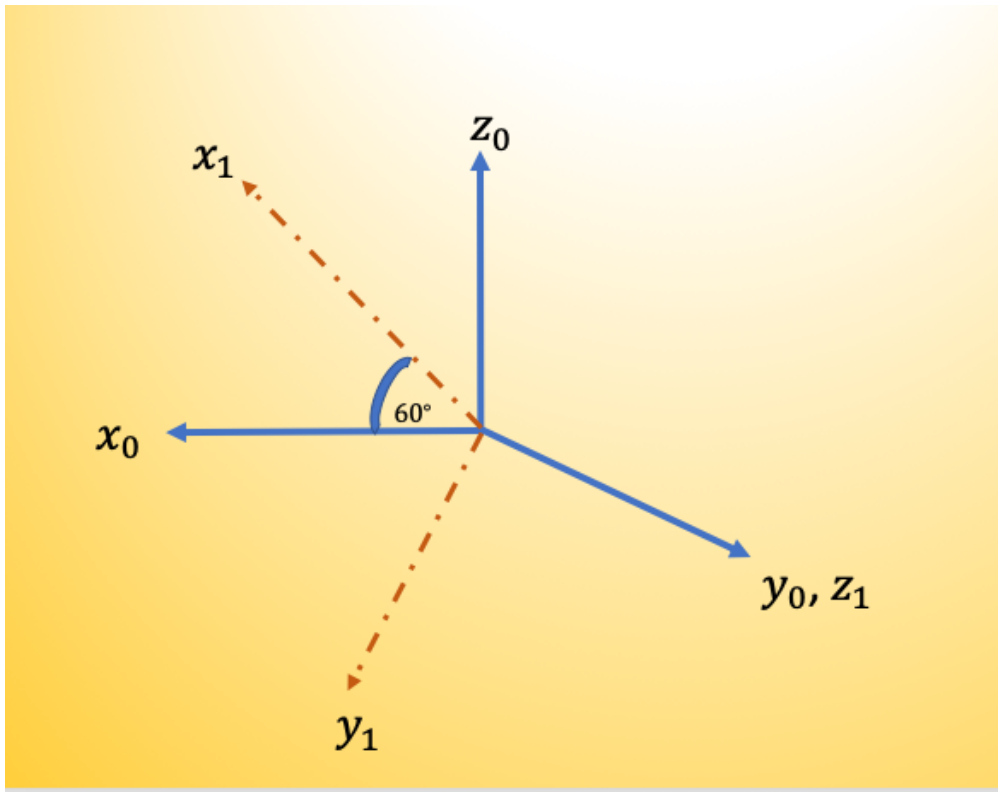


Figure 4.7: Relative orientation between two frames.

**Homework 9.** Compose the rotation matrix in three dimensions where all axes of the inertial frame are rotated by an angle  $\beta$  around each of the  $x_0$ ,  $y_0$  and  $z_0$  axes respectively using the foregoing logic. In addition, for each transformation, verify that (1)  $R_{e,\beta} = I$  where  $e$  is the axes about which we are rotating and  $\beta$  is the angle of rotation, (2) the composition of rotations about the angles  $\beta$  and  $\alpha$  in a successive manner implies that  $R_{z,\beta} R_{z,\alpha} = R_{z,\beta+\alpha}$ , and (3)  $(R_{z,\beta})^{-1} = R_{z,-\beta}$ . Bonus points will be awarded for cool 3D visualizations.

**Homework 10.** For the two frames shown in Fig. 4.7, determine the rotation matrix between them. In addition, explain the difference between rotating about a *current frame* and rotating about a *fixed frame*<sup>3</sup>. In particular, when is it necessary to carry out a *pre-multiplication* and when is it necessary to carry out a *post-multiplication* when transforming points or vectors about coordinate frames?

---

<sup>3</sup>See sections 2.4.1 and 2.4.2 of Spong's book.

### Order of rotations

A rotation about a fixed axis necessarily means a **pre-multiplication** while a rotation about a current axis necessitates a *post-multiplication*.

#### 4.4.5 Composition of Rotations

Rotations matrices have this desirable property that they can be composed together to form transform a point between successive frames. Take for example a frame  $K$  whose orientation relative to frame  $J$  is  $R_{jk}$ , and frame  $J$  whose orientation relative to frame  $I$  is  $R_{ij}$ , we can write out the orientation of frame  $K$  relative to  $I$  as

$$R_{ik} = R_{ij}R_{jk}. \quad (4.4.22)$$

The rotation described above would be equivalent to rotating frame  $K$  relative to frame  $I$  according to  $R_{ij}$ , then aligning frame  $J$  to  $K$ , we rotate  $K$  relative to  $I$  according to  $R_{jk}$ . The resulting frame  $K$  has orientation with respect to  $I$  given by  $R_{ij}R_{jk}$ . This frame relative to which rotation occurs is termed the *current frame*.

**Homework 11.** For the robot manipulator we are using in this class, suppose that you have the following point in the base frame of the robot,  $q_o = [-2, 3, 1]$ . Furthermore, suppose that the joint angles for all six joints are respectively  $\{-90, 60, 30, 45, 90, 125\}$ , transform the point  $q_0$  in the base frame to a coordinate frame on the sixth joint.

### Properties of Rigid Body Rotation Matrices

*Rigid body* rotations preserve

- distance:  $\|Rq - Rp\| = \|q - p\|$  for all  $q, p \in \mathbb{R}^3$
- orientations:  $R(i \times j) = Ri \times Rj$  for all  $i, j \in \mathbb{R}^3$ .

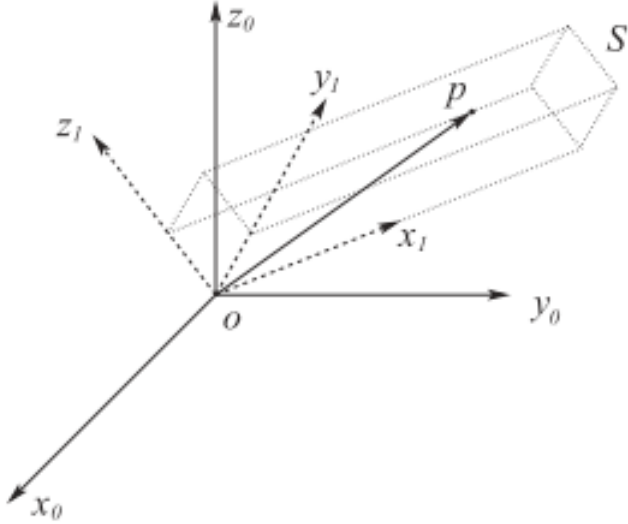


Figure 4.8: Coordinate frames on a body. Reprinted from ([Spong et al., 2006](#))

What follows is adapted from Figure 2.5 from Spong and Vidyasagar's book. It is meant to illustrate the rotation applied to a point from one frame to another.

For consider Fig. 4.8 whereupon the rigid body  $S$  has a coordinate frame  $o_1x_1y_1$  attached. For the coordinates of the point  $p$  with respect to frame  $o_1x_1y_1$  or  $p^1$ , we are tasked with finding the coordinates of  $p$  relative to a fixed reference frame  $o_0x_0y_0$ . We note that  $p^1 = [u, v, w]^T$  satisfies

$$p = ux_1 + vy_1 + wz_1. \quad (4.4.23)$$

Matter-of-factly, the coordinates of  $p^0$  can be obtained based on the projection trick we introduced earlier by projecting  $p$  onto the coordinate axes of  $o_0x_0y_0z_0$  so that we have

$$p^0 = \begin{pmatrix} p \cdot x_0 \\ p \cdot y_0 \\ p \cdot z_0 \end{pmatrix} \quad (4.4.24)$$

so that substituting (4.4.23) into (4.4.24), we have

$$p^0 = \begin{pmatrix} (ux_1 + vy_1 + wz_1) \cdot x_0 \\ (ux_1 + vy_1 + wz_1) \cdot y_0 \\ (ux_1 + vy_1 + wz_1) \cdot z_0 \end{pmatrix} = \begin{pmatrix} x_1 \cdot x_0 & y_1 \cdot x_0 & z_1 \cdot x_0 \\ x_1 \cdot y_0 & y_1 \cdot y_0 & z_1 \cdot y_0 \\ x_1 \cdot z_0 & y_1 \cdot z_0 & z_1 \cdot z_0 \end{pmatrix} \begin{pmatrix} u \\ v \\ w \end{pmatrix} \quad (4.4.25)$$

which upon inspection turns out to be a multiplication of the rotation matrix that transforms point  $p^1$  to point  $p^0$  i.e.

$$p^0 = R_1^0 p^1, \quad (4.4.26)$$

implying that the rotation matrix not only serves to represent the relative orientation of coordinate frames with respect to one another but to transform coordinates of a point from one frame to another.

Finally, we define a similarity transformation *as the matrix representation of a general linear transformation that is transformed from one frame to another*. So if  $I$  is the matrix representation of a linear transformation in a frame  $o_0x_0y_0z_0$  and  $J$  is the equivalent transformation in  $o_1x_1y_1z_1$  then  $I$  and  $J$  are related by

$$J = (R_1^0)^{-1} A R_1^0 \quad (4.4.27)$$

where  $R_1^0$  is the coordinate transformation between frames  $o_1x_1y_1z_1$  and  $o_0x_0y_0z_0$ .

**Lab Exercise:** Carry out a similarity transformation in the elbow frame ( $o_1x_1y_1z_1$ ) of the manipulator with respect to the shoulder frame ( $o_0x_0y_0z_0$ ) when the two frames are related by the rotation

$$R = \begin{pmatrix} 1 & 0 & 0 \\ 0 & -1 & 0 \\ 0 & 0 & 0 \end{pmatrix} \quad (4.4.28)$$

Consider the composition of rotations of Fig. 4.9 where we first rotate by an angle  $\theta$  about the  $x$  axis and then rotate about an angle  $\psi$  about the  $z$  axis. The rotation matrix can be composed as

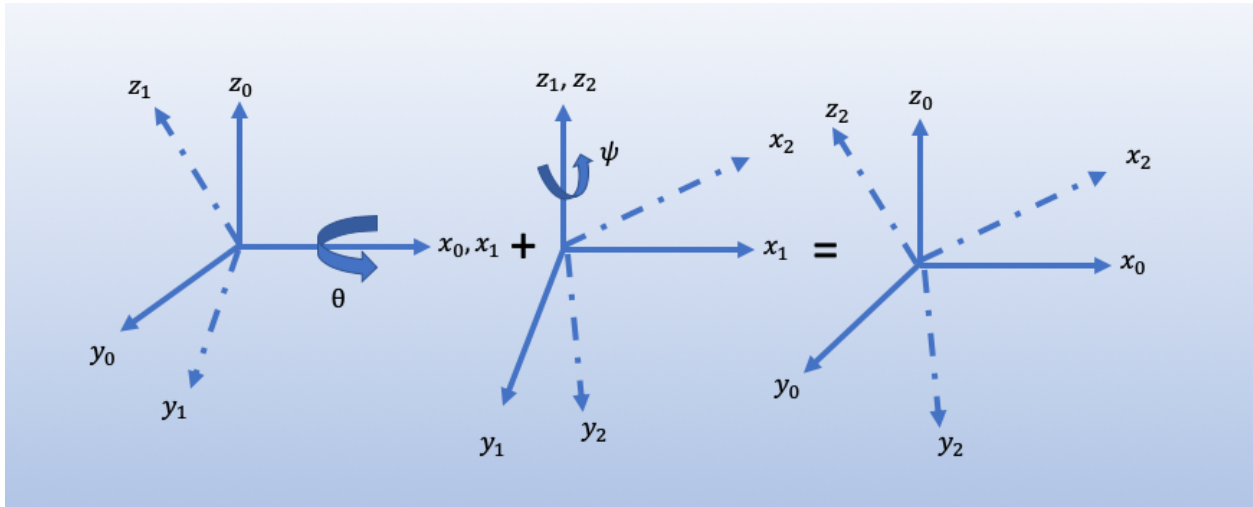


Figure 4.9: Illustration of composition of rotations about a **current axis**.

$$R = R_{x,\theta} R_{z,\psi} = \begin{pmatrix} 1 & 0 & 0 \\ 0 & c_\theta & -s_\theta \\ 0 & s_\theta & c_\theta \end{pmatrix} \cdot \begin{pmatrix} c_\psi & -s_\psi & 0 \\ s_\psi & c_\psi & 0 \\ 0 & 0 & 1 \end{pmatrix} = \begin{pmatrix} c_\psi & -s_\psi & 0 \\ 0 & c_\theta c_\psi & -s_\theta \\ s_\theta s_\psi & s_\theta c_\psi & c_\theta \end{pmatrix} \quad (4.4.29)$$

Notice how the order of multiplication is carried out, owing to the axis about which we are making the transformation.

**Homework 12.** Carry out the transformation above in reverse order. What do you notice?

## 4.5 Parameterization of Rotations $\in SO(3)$

### 4.5.1 Axis-Angle Parameterizations

The exponential coordinates are the *canonical* coordinates of the rotation group. A rigid body has at most three rotational degrees of freedom so that we need at most three variables to denote its orientation in the world. For the matrix

$$R = \begin{bmatrix} r_{11} & r_{12} & r_{13} \\ r_{21} & r_{22} & r_{23} \\ r_{31} & r_{32} & r_{33} \end{bmatrix} \quad (4.5.1)$$

so that equating the foregoing with the exponential map for a rotation about  $\theta$  around an axis  $\omega$  as yields

$$e^{\hat{\omega}\theta} = I + \hat{\omega} \sin \theta + \hat{\omega}^2 (1 - \cos \theta) \quad (4.5.2)$$

$$= \begin{bmatrix} \omega_y^2 v_\theta + c_\theta & \omega_x \omega_y v_\theta - \omega_z s_\theta & \omega_x \omega_z v_\theta + \omega_y s_\theta \\ \omega_x \omega_y v_\theta + \omega_z s_\theta & \omega_y^2 v_\theta + c_\theta & \omega_y \omega_z v_\theta - \omega_x s_\theta \\ \omega_x \omega_z v_\theta - \omega_y s_\theta & \omega_y \omega_z v_\theta + \omega_x s_\theta & \omega_z^2 v_\theta + c_\theta \end{bmatrix}, \quad (4.5.3)$$

where we have used  $v_\theta = 1 - \cos \theta$ . Therefore, we have

$$\text{trace}(R) = r_{11} + r_{22} + r_{33} = 1 + 2c_\theta \quad (4.5.4)$$

Inspecting the matrix of (4.5.3), we have the angle of rotation in terms of the three components of the rotation matrix as

$$\theta = \cos^{-1} \left( \frac{\text{trace}(R) - 1}{2} \right) \quad (4.5.5)$$

where  $\theta$  is defined under the constraint,  $-2\pi n \leq \theta \leq 2\pi n$  owing to the special property of  $R$ .<sup>4</sup>

**Homework 13.** Verify by equating the off-diagonal terms that

$$\omega = \frac{1}{2 \sin \theta} \begin{pmatrix} r_{32} - r_{23} \\ r_{13} - r_{31} \\ r_{21} - r_{12} \end{pmatrix} \quad (4.5.6)$$

suppose  $\theta \neq 0$ . Equation (4.5.5) together with (4.5.6) are what we call the *axis-angle representation*.

## 4.5.2 Euler Angles

The *Euler Angles* are particularly useful for specifying the orientation of a coordinate frame  $J$  with respect to  $I$ . To do this, we start as follows (see Fig. 4.10 for reference):

---

<sup>4</sup>Since  $R$  preserves lengths and  $\det R = +1$ , the eigenvalues of  $R$  have a unit magnitude and occur in complex conjugate pairs. This implies  $-1 \leq \text{trace}(R) \leq 3$

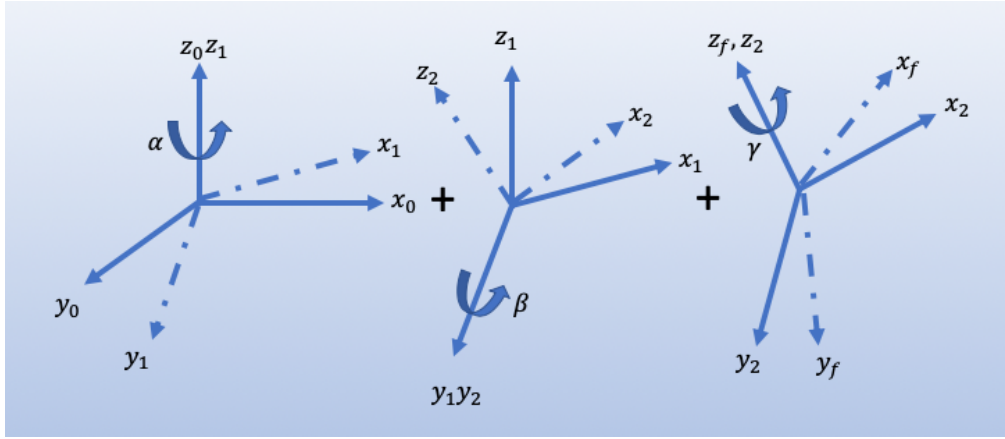


Figure 4.10: An illustration of the ZYZ rotation angles

- we orientate frame  $J$  with frame  $I$  so that the two frames are coincident by rotating by the  $z$  axis about an angle  $\alpha$ ;
- we then rotate about the *new*  $y$ -axis of  $J$  by an angle  $\beta$ ;
- lastly, we rotate about the new  $z$ -axis of rge frame  $J$  by an angle  $\gamma$

so that altogether, we have a rotation  $R_{ij}(\alpha, \beta, \gamma)$  given as

$$R_{ij}(\alpha, \beta, \gamma) = R_z(\alpha)R_y(\beta)R_z(\gamma) \quad (4.5.7)$$

$$\begin{aligned} &= \begin{bmatrix} c_\alpha & -s_\alpha & 0 \\ s_\alpha & c_\alpha & 0 \\ 0 & 0 & 1 \end{bmatrix} \begin{bmatrix} c_\theta & 0 & s_\theta \\ 0 & 1 & 0 \\ -s_\theta & 0 & c_\theta \end{bmatrix} \\ &= \begin{bmatrix} c_\alpha c_\beta c_\gamma - s_\alpha s_\gamma & -c_\alpha c_\beta s_\gamma - s_\alpha c_\gamma & c_\alpha s_\beta \\ s_\alpha c_\beta c_\gamma + c_\alpha s_\gamma & -s_\alpha c_\beta s_\gamma + c_\alpha c_\gamma & s_\alpha s_\beta \\ -s_\beta c_\gamma & s_\beta s_\gamma & c_\beta \end{bmatrix} \quad (4.5.8) \end{aligned}$$

where as before the abbreviations  $c_\alpha, s_\alpha$  are abbreviations for  $\cos \alpha$  and  $\sin \alpha$ . Euler angles arise when we need to recover the  $\alpha, \beta, \gamma$  angles from (4.5.8). Suppose that  $r_{13}$  and  $r_{23}$  are both  $\neq 0$ , we

find that  $c_\beta \neq \pm 1$  and thus with the knowledge that  $\sin \beta > 0$  given (4.5.9a), we find that ,

$$\beta = \arctan 2(r_{33}, \sqrt{1 - r_{33}^2}) \quad (4.5.9a)$$

$$\alpha = \arctan 2(r_{23}/\sin \beta, r_{13}/\sin \beta) \quad (4.5.9b)$$

$$\gamma = \arctan 2(r_{32}/\sin \beta, -r_{31}/\sin \beta) \quad (4.5.9c)$$

where  $\arctan 2(y, x)$  computes  $\tan^{-1}(y/x)$ , determining the quadrant of the angle based on the sign of  $x$  and  $y$ . When  $\sin \beta < 0$ , we find that

$$\beta = \arctan 2(r_{33}, -\sqrt{1 - r_{33}^2}) \quad (4.5.10a)$$

$$\alpha = \arctan 2(-r_{23}/\sin \beta, -r_{13}/\sin \beta) \quad (4.5.10b)$$

$$\gamma = \arctan 2(-r_{32}/\sin \beta, r_{31}/\sin \beta) \quad (4.5.10c)$$

implying that *the Euler angles are not unique* owing to the sign of the angle about which the  $y$  axis rotates.

**Homework 14.** What happens when  $r_{13} = r_{23} = 0$ ? Can you write out the rotation matrix as well as the euler angles for this situation?

In the scenario that results from homework viii, there will be infinitely many solution owing to the fact that only  $\alpha + \beta$  only can be determined. This infinite solutions occur when  $R = I$  and an example scenario of when this occurs is when  $(\alpha, 0, -\alpha)$ .

Using the  $ZYZ$  angles are not the only way of parameterizing the rotation matrix. We could permute the order of rotation or rotate successively about different axis. Examples include  $ZYX$  axes rotations (or Fick angles) and the  $YZX$  axes parameterization or Helmholtz angles. In general robotics speak, note that the *ZYX angles are otherwise referred to as the yaw, pitch and roll angles, wherein the rotation matrix  $R_{ij}$  is defined by rotating about the  $x$ -axis in the body frame (roll), then the  $y$ -axis in the body frame (pitch), and finally the  $z$ -axis in the body frame (yaw)*. An advantage of the Fick angle and Helmholtz angle parameterization is that they avoid singularity at  $R = I$  though they do contain singularities at other configurations.

### 4.5.3 Quaternions

Rather than use rotation matrices to represent orientations, a more effective approach of representing orientations are *quaternions*. Instead of locally parameterizing the  $SO(3)$  Lie group, quaternions, unlike rotation matrices, globally parameterize the  $SO(3)$  Lie Group. Formally, we represent a quaternion as follows:

$$Q = q_0 + q_x \mathbf{i} + q_y \mathbf{j} + q_z \mathbf{k}, \quad q_{\{i=0,\dots,3\}} \in \mathbb{R} \quad (4.5.11)$$

where  $q_0$  is the scalar component of  $Q$  and  $\mathbf{q} = (q_x, q_y, q_z)$  is the vector component.

The *unit quaternions* are the subset of all  $Q \in \mathbb{Q}$  such that  $\|Q\| = 1$ ; for a rotation matrix  $R = \exp(\hat{\omega}\theta)$ , we have the unit quaternion as

$$Q = (\cos(\theta/2), \omega \sin(\theta/2)), \quad (4.5.12)$$

where  $\omega \in \mathbb{R}^3$  is the axis of orientation and  $\theta \in \mathbb{R}$  is the angle of rotation.

#### Summary of Parameterizations

Rotation matrices can be parameterized in one of many ways depending on our use case.

The common examples of parameterizations are

- (1) Axis-Angle representation;
- (2) Euler angles ( $ZYZ$ ) representation;
- (3) Fick angles (*i.e.*  $ZYX$  or yaw, pitch and roll) representation;
- (4) Helmholtz angles (or  $YZX$ ) angles representation; and
- (5) Quaternions.

## 4.6 Homogeneous Coordinates

For a point  $q \in \mathbb{R}^3$ , we represent the *homogeneous coordinates* of point  $q$  as

$$\bar{q} = \begin{pmatrix} q_x & q_y & q_z & 1 \end{pmatrix}^T \quad (4.6.1)$$

whose origin has the following coordinates

$$\bar{O} = \begin{pmatrix} 0 & 0 & 0 & 1 \end{pmatrix}^T. \quad (4.6.2)$$

For vectors, it would suffice for us to write

$$\bar{v} = \begin{pmatrix} v_x & v_y & v_z & 0 \end{pmatrix}^T \quad (4.6.3)$$

where the last element is zero because a vector is the difference of two points.

### Vectors and Points

- The sum or difference of two vectors results in a vector
- The difference between two points is a vector
- The sum of two points do not exist

We now define the homogeneous transformation of a point  $q_j$  in frame  $J$  with respect to a coordinate frame  $I$  with  $p_{ij}$  being the distance between  $q_i$ , and  $q_j$ , and  $R_{ij}$  being the rotation matrix that transforms points in frame  $J$  to points in frame  $I$ . We write

$$q_i = p_{ij} + R_{ij}q_j \quad (4.6.4)$$

or more appropriately

$$\begin{pmatrix} q_i \\ 1 \end{pmatrix} = \begin{pmatrix} R_{ij} & p_{ij} \\ 0 & 1 \end{pmatrix} \begin{pmatrix} q_j \\ 1 \end{pmatrix} \quad (4.6.5)$$

which implies that  $\bar{q} = \bar{g}_{ij}\bar{q}_j$ . We say  $\bar{g}_{ij}$  is the *homogeneous representation* of  $g_{ij} \in SE(3)$ .

Similar to rotation matrices, rigid body transformation matrices can be composed to form new rigid body transformations. So, suppose we have the  $g_{jk}$  which is the transformation of a body  $K$  relative to body  $J$  and  $g_{ij}$  which is the transformation of body  $J$  relative to body  $I$ , then we can

find the configuration of  $K$  relative to  $I$  as follows

$$\bar{g}_{ik} = \bar{g}_{ij}\bar{g}_{jk} = \begin{pmatrix} R_{ij} & p_{ij} \\ 0 & 1 \end{pmatrix} \begin{pmatrix} R_{jk} & p_{jk} \\ 0 & 1 \end{pmatrix} \quad (4.6.6)$$

$$= \begin{pmatrix} R_{ij}R_{jk} & R_{ij}p_{jk} + p_{ij} \\ 0 & 1 \end{pmatrix}. \quad (4.6.7)$$

Since (4.6.7) is a form of (4.3.4), we conclude that the composition of rigid body transformations and  $I_{4 \times 4}$  is in the special Euclidean group as well. In addition,

$$g^{-1} = (R^T p, R^T). \quad (4.6.8)$$

## 4.7 Rigid Body Velocities

We are concerned with the velocity of a rigid body with motion described by a time-parameterized curve  $g(t) \in SE(3)$ . For a start, we will consider the trajectory motion of an object frame  $J$  whose origin is at a frame  $I$  and it is rotating relative to the fixed frame  $I$ . We call frame  $I$  the *spatial frame* and the frame  $J$ , the *body frame*.

### 4.7.1 Rotational Velocities

For a point  $q$  whose coordinates  $q_j$  are fixed in the body frame, a path in spatial coordinates is followed given by

$$q_i(t) = R_{ij}(t)q_j. \quad (4.7.1)$$

The velocity in spatial coordinates is

$$v_{q_i}(t) = \frac{\partial}{\partial t} q_i(t) = \dot{R}_{ij}(t)q_j. \quad (4.7.2)$$

We see that  $\dot{R}_{ij}$  maps the body coordinates,  $q_j$  to the spatial velocity of  $q$ . We would like to develop a more compact representation of the orientation of the point  $q$  relative to the spatial frame  $I$  by

exploiting the special structure of  $\dot{R}_{ij}$ . Thus, we write

$$v_{q_i}(t) = \dot{R}_{ij}(t) R_{ij}^{-1}(t) R_{ij}(t) q_j. \quad (4.7.3)$$

We define the *instantaneous spatial angular velocity*  $\hat{\omega}_{ij}^s \in \mathbb{R}^3$  as seen in the spatial frame  $I$  as

$$\hat{\omega}_{ij}^s(t) = \dot{R}_{ij}(t) R_{ij}^{-1}(t) \quad (4.7.4)$$

and we define the *instantaneous body angular velocity* as seen in the body frame  $J$  as

$$\hat{\omega}_{ij}^b(t) = R_{ij}^{-1}(t) \dot{R}_{ij}(t) \quad (4.7.5)$$

We define the body angular velocity as viewed from the instantaneous body frame  $J$  as

$$\hat{\omega}_{q_b}^b = R_{ij}^{-1} \hat{\omega}_{ij}^s R_{ij}, \text{ or } \hat{\omega}_{ij}^b = R_{ij}^{-1} \hat{\omega}_{ij}^s, \quad (4.7.6)$$

so that the body angular velocity can be recovered from the spatial angular velocity by rotating the angular velocity vector into the instantaneous body frame. Thus, (4.7.3) becomes

$$v_{q_i}(t) = \hat{\omega}_{ij}^s(t) R_{ij}(t) q_j = \hat{\omega}_{ij}^s(t) \times q_i(t) \quad (4.7.7)$$

Similarly, the velocity in the frame  $J$  can be derived from (4.7.1) as

$$q_j = R_{ij}^{-1}(t) q_i(t) \quad (4.7.8a)$$

$$v_{q_j}(t) = \dot{R}_{ij}^T(t) v_{q_i}(t) = \omega_{ij}^b(t) \times q_j. \quad (4.7.8b)$$

Thus we have the compact description of the rigid body particles' velocities in both the body and spatial angular frames as  $\omega_{ij}^b$  and  $\hat{\omega}_{ij}^s$ .

**Homework 15.** Consider the motion of a point body about the  $x$  axis of an orthogonal triad with respect to a certain spatial frame located at  $O(0, 0, 0)$ . Determine the body and spatial velocities of the point with respect to the origin,  $O$ .

### 4.7.2 Rigid Body Velocity

We shall denote the rigid body motion of a frame  $J$  attached to a body so that is it fixed relative to a frame  $I$  by  $g_{ij}(t)$ . We write the velocity in the spatial frame as  $\dot{g}_{ij}g_{ij}^{-1}$  which is symbolically  $(\dot{p}_{ij}, \dot{R}_{ij}) \cdot (R_{ij}^T, -R_{ij}^T p_{ij})$  following the notation we introduced in (4.6.8). This has an isomorphism of a twist and it is given by

Twist in Spatial Frame

$$\eta_{ij}^s = \dot{g}_{ij}g_{ij}^{-1} = \begin{bmatrix} \omega_{ij}^s & v_{ij}^s \\ 0 & 0 \end{bmatrix} = \begin{bmatrix} \dot{R}_{ij}R_{ij}^T & -\dot{R}_{ij}R_{ij}^T p_{ij} + \dot{p}_{ij} \\ 0 & 0 \end{bmatrix} \in \mathfrak{se}(3) \quad (4.7.9)$$

whereupon the twist coordinates  $\xi^s \in \mathbb{R}^6$  in the body frame can be recovered as

$$\begin{pmatrix} v_{ij}^s \\ \omega_{ij}^s \end{pmatrix} = \begin{pmatrix} -\dot{R}_{ij}R_{ij}^T p_{ij} + \dot{p}_{ij} \\ (\dot{R}_{ij}R_{ij}^T)^\vee \end{pmatrix} \quad (4.7.10)$$

Similarly, in body coordinates, we find that the twist is given by

Twist in Body Frame

$$\eta_{ij}^b = g_{ij}^{-1}\dot{g}_{ij} = \begin{bmatrix} \omega_{ij}^b & v_{ij}^b \\ 0 & 0 \end{bmatrix} = \begin{bmatrix} \dot{R}_{ij}R_{ij}^T & R_{ij}^T p_{ij} \dot{p}_{ij} \\ 0 & 0 \end{bmatrix} \in \mathfrak{se}(3) \quad (4.7.11)$$

whereupon the twist coordinates  $\xi^b \in \mathbb{R}^6$  in the body frame can be recovered as

$$\begin{pmatrix} v_{ij}^b \\ \omega_{ij}^b \end{pmatrix} = \begin{pmatrix} -\dot{R}_{ij}^T \dot{p}_{ij} \\ (R_{ij}^T \dot{R}_{ij})^\vee \end{pmatrix} \quad (4.7.12)$$

Furthermore, we have that

$$\eta_{ij}^s = \begin{pmatrix} -\dot{R}_{ij} & \hat{p}_{ij}R_{ij} \\ 0 & R_{ij} \end{pmatrix} \begin{pmatrix} v_{ij}^b \\ \omega_{ij}^b \end{pmatrix}. \quad (4.7.13)$$

**Homework 16.** Confirm equations (4.7.9), (4.7.11) and (4.7.13).

The matrix which transforms from the body coordinate frame to the spatial velocity frame is the so-called *adjoint transformation* of  $g$  (c.f. Fig. 4.2), defined as

$$Ad_g = \begin{pmatrix} R & \hat{p}R \\ 0 & R \end{pmatrix} \quad (4.7.14)$$

and whose inverse is given by

$$Ad_g^{-1} = \begin{pmatrix} R^T & -(R^T p)^\wedge R^T \\ 0 & R^T \end{pmatrix} = \begin{pmatrix} R^T & -R^T \hat{p} \\ 0 & R^T \end{pmatrix} = Ad_{g^{-1}} \quad (4.7.15)$$

## REFERENCES

- Ball, R. S. (1908). *A Treatise on the Theory of Screws*. Cambridge university press. [39](#)
- Bern, J. M., K.-H. Chang, and S. Coros (2017). Interactive design of animated plushies. *ACM Transactions on Graphics (TOG)* 36(4), 80. [25](#)
- Besl, P. J. and N. D. McKay (1992). Method for registration of 3-d shapes. In *Sensor fusion IV: control paradigms and data structures*, Volume 1611, pp. 586–606. International Society for Optics and Photonics. [5](#)
- Bishop-Moser, J., G. Krishnan, C. Kim, and S. Kota (2012). Design of soft robotic actuators using fluid-filled fiber-reinforced elastomeric enclosures in parallel combinations. In *2012 IEEE/RSJ International Conference on Intelligent Robots and Systems*, pp. 4264–4269. IEEE. [25](#)
- Giorelli, M., F. Renda, M. Calisti, A. Arienti, G. Ferri, and C. Laschi (2015). Neural Network And Jacobian Method For Solving The Inverse Statics Of A Cable-driven Soft Arm With Nonconstant Curvature. *IEEE Transactions on Robotics* 31(4), 823–834. [27](#)
- Gough, V. (1957). Contribution to discussion of papers on research in automobile stability, control and tyre performance. *Proc. of Auto Div. Inst. Mech. Eng.* 171, 392–395. [31](#)
- Hannan, M. W. and I. D. Walker (2000). Novel Kinematics for Continuum Robots. pp. 227–238. *Advances in Robot Kinematics*. [27](#)
- Hannan, M. W. and I. D. Walker (2003). Kinematics and the Implementation of an Elephant’s Trunk Manipulator and Other Continuum Style Robots. *Journal of Robotic Systems* 20(2), 45–63. [27](#)

Hopkins, J. B., J. Rivera, C. Kim, and G. Krishnan (2015). Synthesis and analysis of soft parallel robots comprised of active constraints. *Journal of Mechanisms and Robotics* 7(1), 011002. [iv](#), [26](#)

Horn, B. K. (1987). Closed-form solution of absolute orientation using unit quaternions. *Josa a* 4(4), 629–642. [12](#)

Hunt, K. H. (1977). *Kinematic Geometry of Mechanisms*. Oxford University Press. [iv](#), [25](#), [33](#), [34](#)

Hunt, K. H. (1983). Structural Kinematics of In- Parallel-Actuated Robot-Arms. *105*(December 1983), 705–712. [iv](#), [29](#)

Kabsch, W. (1978). A discussion of the solution for the best rotation to relate two sets of vectors. *Acta Crystallographica Section A* 34(5), 827–828. [6](#), [12](#)

Merlet, J. (2015). *Parallel robots*. Springer. [31](#), [32](#)

Murray, R. M. (1994). *A Mathematical Introduction To Robotic Manipulation*. CRC press. [33](#), [47](#)

Ogunmolu, O. (2019a). Kinematics and Dynamics of an In-Parallel-Actuated Soft Robot Manipulator: Application to Cranial Cancer Radiosurgery. [27](#)

Ogunmolu, O., A. Kulkarni, Y. Tadesse, X. Gu, S. Jiang, and N. Gans (2017). Soft-NeuroAdapt: A 3-DOF Neuro-Adaptive Patient Pose Correction System for Frameless and Maskless Cancer Radiotherapy. In *IEEE/RSJ International Conference on Intelligent Robots and Systems (IROS)*, *Vancouver, BC, CA*, pp. 3661–3668. IEEE. [27](#)

Ogunmolu, O., X. Liu, N. Gans, and R. Wiersma (2020). Mechanism and Constitutive Model of a Continuum Robot for Head and Neck Cancer Radiotherapy. In *Accepted at IEEE International Conference on Robotics and Automation (ICRA), Paris, France*. [27](#)

Ogunmolu, O. P. (2019b). *A Multi-DOF Soft Robot Mechanism for Patient Motion Correction and Beam Orientation Selection in Cancer Radiation Therapy*. Ph. D. thesis, The University of Texas at Dallas; UT Southwestern Medical Center. [27](#)

Ogunmolu, O. P., X. Gu, S. Jiang, and N. R. Gans (2015). A Real-Time, Soft Robotic Patient Positioning System for Maskless Head and Neck Cancer Radiotherapy: An Initial Investigation. In *Automation Science and Engineering (CASE), 2015 IEEE International Conference on, Gothenburg, Sweden*, pp. 1539–1545. IEEE. [27](#)

Ogunmolu, O. P., X. Gu, S. Jiang, and N. R. Gans (2016). Vision-based Control of a Soft Robot for Maskless Head and Neck Cancer Radiotherapy. In *Automation Science and Engineering (CASE), 2016 IEEE International Conference on, Fort Worth, Texas*, pp. 180–187. IEEE. [27](#)

Renda, F., M. Giorelli, M. Calisti, M. Cianchetti, and C. Laschi (2014). Dynamic model of a multibending soft robot arm driven by cables. *IEEE Transactions on Robotics* 30(5), 1109–1122. [27](#)

Renda, F. and L. Seneviratne (2018). A Geometric and Unified Approach for Modeling Soft-Rigid Multi-body Systems with Lumped and Distributed Degrees of Freedom. *2018 IEEE International Conference on Robotics and Automation (ICRA)*, 1567 – 1574. [27](#)

Shepherd, R. F., F. Ilievski, W. Choi, S. A. Morin, A. A. Stokes, A. D. Mazzeo, X. Chen, M. Wang, and G. M. Whitesides (2011). Multigait soft robot. *Proceedings of the National Academy of Sciences* 108(51), 20400–20403. [27](#)

Spong, M. W., S. A. Hutchinson, and M. Vidyasagar (2006). Robot modeling and control. *IEEE Control Systems* 26(6), 113–115. [iv](#), [36](#), [58](#)

Stewart, D. (1965). A platform with six degrees of freedom. *Proceedings of the institution of mechanical engineers* 180(1), 371–386. [31](#)

Weisstein, E. W. Homeomorphic. [6](#)